RSC Advances

REVIEW

View Article Online
View Journal | View Issue

Cite this: *RSC Adv.*, 2020, **10**, 36058

Recent advances in additive manufacturing of engineering thermoplastics: challenges and opportunities

Maisyn Picard, [ab] Amar K. Mohanty [*ab] and Manjusri Misra [*ab]

Received 1st June 2020
Accepted 17th August 2020

DOI: 10.1039/d0ra04857g

rsc.li/rsc-advances

There are many limitations within three-dimensional (3D) printing that hinder its adaptation into industries such as biomedical, cosmetic, processing, automotive, aerospace, and electronics. The disadvantages of 3D printing include the inability of parts to function in weight-bearing applications, reduced mechanical performance from anisotropic properties of printed products, and limited intrinsic material performances such as flame retardancy, thermal stability, and/or electrical conductivity. Many of these shortcomings have prevented the adaptation of 3D printing into product development, especially with few novel researched materials being sold commercially. In many cases, high-performance engineering thermoplastics (ET) provide a basis for increased thermal and mechanical performances to address the

[a]*School of Engineering, University of Guelph, Thornbrough Building, Guelph, N1G 2W1, ON, Canada. E-mail: mohanty@uoguelph.ca; mmisra@uoguelph.ca*

[b]*Bioproducts Discovery and Development Centre, Department of Plant Agriculture, University of Guelph, Crop Science Building, Guelph, N1G 2W1, ON, Canada*

Maisyn Picard has completed her Bachelor's degree in Biomedical Engineering (with distinction) from the University of Guelph. Currently, she has completed her Master of Applied Science degree under the advice of Professor Amar Mohanty and Professor Manjusri Misra in Biological Engineering at the University of Guelph (Guelph, Ontario, Canada). Ms Picard's research interests include additive manufacturing, polymer processing and characterization, and sustainable materials development via a circular economic approach.

Dr Amar Mohanty is a Professor and OAC Distinguished Research Chair in Sustainable Biomaterials and holds a University Research Leadership Chair at the University of Guelph. He is an international leader in the field of biomaterials with a focus on engineering new sustainable materials. Prof. Mohanty's research interests have focused on the bioeconomy related to bioplastics, biobased materials, and sustainable composites. He has more than 800 publications to his credit, including 396 peer-reviewed journal papers and 61 patents awarded/applied. He has 34399 citations of his research with an h-index of 83 (Google Scholar). Prof. Mohanty has received many awards, including the JL White Innovation Award from the Polymer Processing Society; Synergy Award for Innovation from Natural Sciences and Engineering Research Council of Canada (NSERC); Lifetime Achievement Award from the BioEnvironmental Polymer Society (BEPS); Andrew Chase Forest Products Division Award from the American Institute of Chemical Engineers (AIChE) and OAC Alumni Distinguished Researcher Award. Prof. Mohanty has been named a Fellow of the American Institute of Chemical Engineers, a Fellow of Royal Society of Chemistry (UK) and a Fellow of the Society of Plastic Engineers. Prof. Mohanty is the Editor-in-Chief of Sustainable Composites, Composites Part C: Open Access.

shortcomings or limitations of both selective laser sintering and extrusion 3D printing. The first strategy to combat these limitations is to fabricate blends or composites. Novel printing materials have been implemented to reduce anisotropic properties and losses in strength. Additives such as flame retardants generate robust materials with V0 flame retardancy ratings, and compatibilizers can improve thermal or dimensional stability. To serve the electronic industry better, the addition of carbon black at only 4 wt%, to an ET matrix has been found to improve the electrical conductivity by five times the magnitude. Surface modifications such as photopolymerization have improved the usability of ET in automotive applications, whereas the dynamic chemical processes increased the biocompatibility of ET for medical device materials. Thermal resistant foam from polyamide 12 and fly ash spheres were researched and fabricated as possible insulation materials for automotive industries. These works and others have not only generated great potential for additive manufacturing technologies, but also provided solutions to critical challenges of 3D printing.

Dr Manju Misra is a Professor at the School of Engineering and holds a joint appointment in the Dept. of Plant Agriculture at the University of Guelph. She is also the Research Program Director of the Plant – Technology Panel for the Ontario Agri-Food Innovation Alliance, a program between the Ontario Ministry of Agriculture and Rural Affairs (OMAFRA) and the University of Guelph. She is a Fellow of the Royal Society of Chemistry (UK) and the American Institute of Chemical Engineers (AIChE). Dr Misra's current research focuses primarily on novel bio-based composites and nanocomposites from agricultural, forestry and recycled resources for the sustainable bio-economy moving towards a circular economy. She has authored more than 700 publications, including 369 peer-reviewed journal papers, 21 book chapters, and 51 patents. She was an editor of the CRC Press volume, "Natural Fibers, Biopolymers and Biocomposites", Taylor & Francis Group, Boca Raton, FL (2005); American Scientific Publishers volume "Packaging Nanotechnology", Valencia, California (2009); "Polymer Nanocomposites", Springer (2014) and "Fiber Technology for Fiber-Reinforced Composites", Woodhead Publishing (2017). She was the chief editor of "Biocomposites: Design and Mechanical Performance" Woodhead Publishing (2015). She was the President of the BioEnvironmental Polymer Society (BEPS) in 2009. She serves on the editorial board of "Journal of Applied Polymer Science", "Composites Part A: Science and Manufacturing", "Polymer Testing", and "Composites Part C: Open Access". In 2012, Dr Misra received the prestigious "Jim Hammar Memorial Award" from BEPS and University of Guelph's Innovation of the year award in 2016 for her involvement in developing the "Compostable single-serve coffee pods". In 2017, Professor Misra also received the Andrew Chase Division Award in Chemical Engineering from the Forest Bioproducts Division of AIChE. In 2019, Professor Misra was awarded the Woman of Distinction in Science, Technology, Engineering & Math (STEM) from the Guelph YWCA-YMCA. Total citations: 32818; h-index: 81; i10-index: 345 (Google Scholar, July 23, 2020).

1. Introduction

Currently, the additive manufacturing (AM) market is in demand for a larger variety of feedstock materials with novel thermal, mechanical, electrical, or biocompatible characteristics. In this review, feedstock materials refer to those that are commercially available for industries for the use of printing. The addition of more printing materials with unique mechanical performances might better serve wider range of applications and industries that currently cannot implement the AM technologies. A comprehensive review of the current market solutions discovered in academia could bridge this knowledge gap for industry and suggest novel materials. Three-dimensional (3D) printing is an additive manufacturing process where complex geometric parts can be made in a short period of time (*i.e.*, without the need for tools and die fabrication) in a layer-by-layer fashion.[1,2] This technology has reduced the need for machining or tooling products/prototypes, and has resulted in cost and time saving.[3] Since the inception of this technology in 1986, various methods of 3D printing have been created.[4] The most common methods are extrusion 3D printing (E3DP) *i.e.*, fused filament fabrication, big area additive manufacturing, and selective laser sintering (SLS).[4] However, other methods include stereolithography, direct energy deposition, and ink jetting.[3]

Extrusion 3D printing can be further categorized as either small-scale or large-scale printers. Small-scale printers were referred to as fused deposition modelling (FDM) prior to trademarking; however, the same process has been renamed fused filament fabrication (FFF). These desktop-sized printers extrude thermoplastic polymer filaments through a heated nozzle and deposit the extrudate on to a heated bed,[5] building components by the bottom up method. The printer and its products are created at a comparatively low cost to that of SLS.[4] However, the limitations of these printers include a minimal filament diameter and a smaller print area that is limited by the size of the printer's bed. When developing materials, the size constraint of the filament diameter may result in needed additives (increasing costs) or increased time to optimize the processing conditions.[6] However, to overcome these challenges, large-scale extrusion printers were fabricated, which offer the option for pellet or filament feed systems. Big-area-additive-manufacturing (BAAM) is another name for these large scale

extrusion printers[7–9] and they are able to increase the production rates and times in hopes of adapting 3D printing into mass production.

Selective laser sintering, also known as a powder bed fusion process,[10] requires the use of a powder bed and a laser to melt the polymer such that each layer connects to the surrounding ones. This process can generate larger parts than FFF but requires more space and resources to do so; *i.e.*, space for the large powder bed and substantial left-over materials that are not solidified by the laser. The most common thermoplastic used for FFF is poly(lactic acid) (PLA) but its use is limited in SLS due to its thermal stability and mechanical properties.[11] Similarly, SLS is limited to resins or other materials that offer minimal variability in performance.[12] Engineering thermoplastics, as well as blends or composites of engineering thermoplastics, can address some limitations in 3D printing associated with mechanical and thermal performances. However, a limited number of polymers have been investigated and transitioned to industry to date.

Some of the most common printing materials that are commercially available are engineering thermoplastics. Engineering thermoplastics are noteworthy because they provide high mechanical performances and high chemical stability.[13] Some commonly used engineering thermoplastics include PAs (also referred to as polyamides), poly(ether-*block*-amide), polyetherimides (PEIs), polyimides (PIs),[14] and polycarbonates (PCs).[13] Substantial work has been completed in researching engineering thermoplastics for injection and compression molding. Engineering thermoplastics have been used in the automotive industry,[15] the biomedical industry,[16] and many more because of their versatile nature. In some cases, these materials are blended with other polymeric materials to vary the characteristics such as mechanical performance, biocontent, and/or cost.[17]

The use of blending polymers for injection molding practices has been studied extensively since the resulting novel materials display traits that are a combination of both starting materials. Various engineering thermoplastics have been blended to make new materials with tailorable properties. For example, Asadinezhad *et al.*[18] blended poly(trimethylene terephthalate) (PTT) and polyamide (PA)12;[18] PTT and poly(butylene terephthalate) (PBT) were blended for unique performances between those of both neat polymers,[19,20] and PBT/PC blends[21] were studied to determine their unique properties. In some cases, engineering thermoplastics have been blended with commodity polymers. Codou *et al.*[123] examined PA 6/polypropylene blends with the addition of biocarbon to generate thermally stable and sustainable composites.[22] Other sustainable blends include combining PLA and PBT.[23] Blending has been quite successful in injection molding to generate tailor-made, sustainable, or unique materials and the same strategy has provided considerable potential to the 3D printing market as well. Blends of PEI and one of PC or glycol-modified PET (PETG) were studied by Cicala *et al.*[22] The studied materials displayed potential as alternatives to other commercialized PEI polymers or blends such as Ultem 9085, which is a commercially available PEI blend manufactured by Stratasys[22] for fused filament fabrication. Although the material was not tested for its FFF properties, based on the injection molding properties, it was determined that 90PEI/10PC was a prime substitute. The authors determined that the mechanical performance was similar to that of commercially available filaments but obtained at about half the cost.[22]

Once the materials are blended, *via* extrusion or reactive extrusion, they are collected as filaments. The collected filaments can be size-reduced to powder or pellets before use in AM equipment. Since FFF uses filaments without further modifications, the experimental material can be collected immediately following the extrusion process and maintained in filament form. This would be beneficial since no other resources (*i.e.*, time, energy, or labour) would be required to transform the materials.[24] The same is true for the large-scale extrusion 3D printers that operate on a filament system. However, the pellet feed systems underwent the size reduction of filaments prior to use.[7] Although this can be beneficial since it removes the filament diameter limitations as mentioned above, it does require additional energy input and time. This may have an increased associated cost and would have to be investigated by industry prior to use. Experimental materials used in SLS require the most modifications after extrusion. The filaments must be cryomilled to generate fine powders[25] to function well in SLS.

Although the purpose of blending materials is to diversify and optimize particular aspects like mechanical performances,[26] filament consistency,[6] and surface finish.[27] There are other methods to optimize the extrusion output quality as well as print quality. This can be completed through trial-and-error processes, strategic experimental design[28] and tailored printing parameters. Irrespective of the optimization methods, such methods are required to generate complete parts without warpage or delamination and materials with diversified mechanical performances.

Another technique being studied to generate a greater variety of feedstock materials and improved mechanical performance is through the implementation of composite materials. The composites fabricated for 3D printing can vary from lignocellulosic materials[29–31] to carbon-based materials[32] and even inorganic fillers.[33] The combinations of composites, blends, or refined printing materials can assist with the generation of the materials, and 3D printing technology can expand to the 4-dimensional (4D) printing market and fabricate novel products.[34]

The scope of this literature review is to focus on the use of engineering thermoplastics for 3D printing *via* E3DP (small and large scale) and SLS methods. A critical review will summarize what has been done with these materials, how engineering thermoplastics could address some shortcomings of traditional thermoplastics, as well as examine the feasibility of the materials for large-scale production. The optimization and implementation of engineering thermoplastics have the potential to generate feedstock materials with larger variability in mechanical performance. The newly discovered polymers with improved performance can better serve the biomedical, electrical and automotive industries.

2. Methods

2.1 Methods for preparing materials

Filaments are often produced using an extrusion or reactive extrusion (Fig. 1) that operates *via* twin-screw or single-screw configurations. Screws function by either rotating in the same or opposite directions, referred to as counter- or co-rotating. If filaments require a specific diameter for use in 3D printing, then processing conditions such as feed rate, collection rate, screw speed and melt temperature require optimization.[6]

2.2 Methods of 3D printing

There are several methods for 3D printing, which have been implemented to assist the generation of complex designs or prototypes in a short period of time. The most common methods include (1) E3DP, which includes fused filament fabrication (FFF) and big area additive manufacturing (BAAM);[4] (2) selective laser sintering (SLS);[4] (3) stereolithography (SLA);[4] (4) laminated object modelling.[4] Although SLS was the first commercially available process, E3DP and SLS are the more commonly studied AM processes with engineering thermoplastics. The diversity of printing parameters and operational practices offers a unique means of generating complex products over injection or compression molding practices.

2.2.1 Extrusion 3D printing

Fused filament fabrication. Fused filament fabrication is an E3DP method where a filament is extruded through a heated nozzle and placed onto a heated bed/platform (Fig. 2). The molten filament is referred to as the extrudate and is relatively simple to place during the print since the computer-aided design is spliced into layer-by-layer instructions for the printer to follow. For this type of printing, there are many functional materials to be used for a wide range of products functioning in the automotive,[36] electrical[37] and biomedical[38] industries. However, more work is required to generate economically and environmentally-friendly feedstock printing materials. The ease of use of FFF printers has led to their personal use with desktop computers, and a general variety of commercially available feedstocks. However, there are definite drawbacks and limitations to this technology.

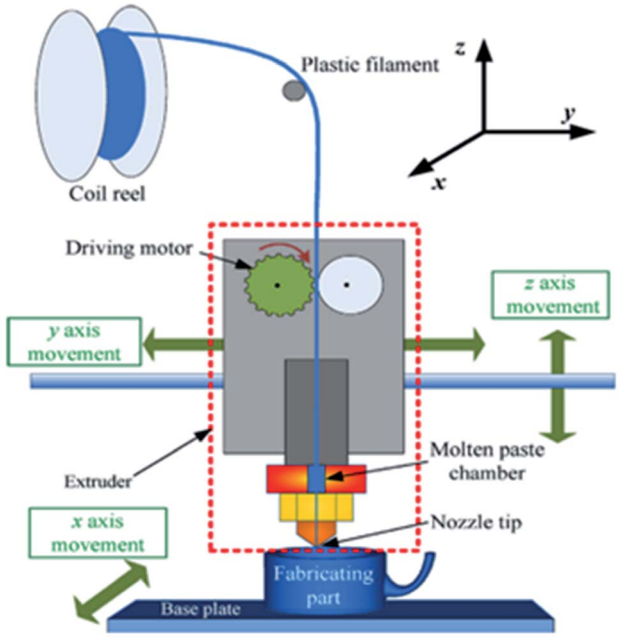

Fig. 2 Schematic representation of fused filament fabrication.[39] Reprinted with permission from Elsevier: *Additive Manufacturing*, Copyright 2020, License: 4743160219820.

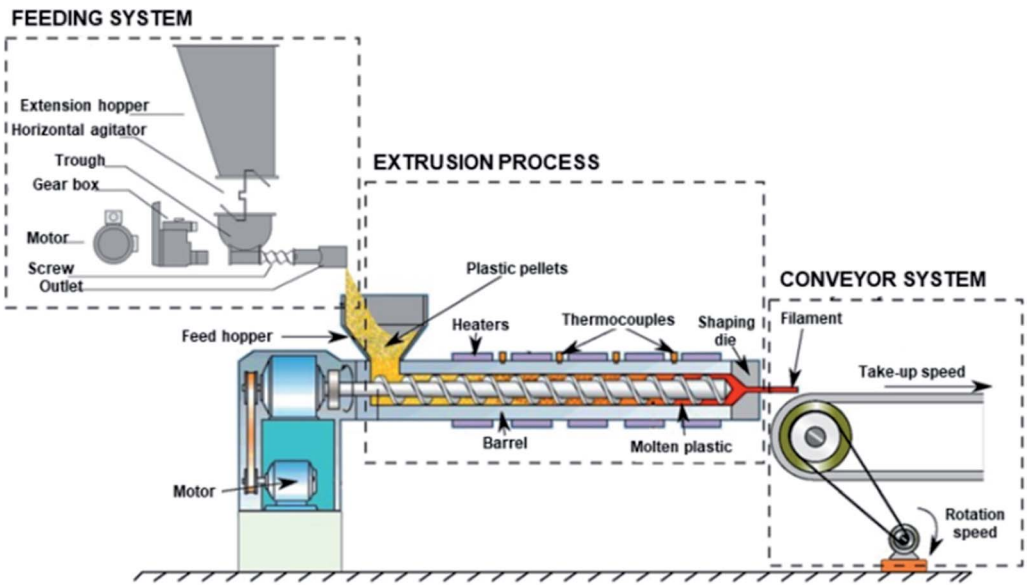

Fig. 1 Extrusion set-up for filament processing.[35] Reprinted with permission from Elsevier: *Additive Manufacturing*, Copyright 2020, License: 4838260364616.

This method of printing requires support for extremely complicated designs with projections above the bed.[4] Unfortunately, the requirements of the support material increase the cost slightly and increase the waste generated. The optimization of prints can reduce waste and time. Other challenges with FFF include (1) limited or specifically supported filament diameters,[37] which can create challenges for new experimental materials for E3DP; (2) relatively small print areas.[8] As a result, an additional method of E3DP has been created and it is referred to as big-area-additive manufacturing.[9]

Big-area additive manufacturing. In industry, large-scale custom printers have been designed for larger volume prints and increased printing speeds.[40] This process of E3DP has been coined big-area-additive manufacturing (BAAM).[41] Unique to BAAM printers is their ability to use either filament feedstocks or pellets to deposit onto the bed. Pellet-based systems require the hopper to be filled with dried pellets and then fed into a heated channel with a single screw inside. The channel for the polymers is often covered in thermal jackets and monitored by thermocouples. The heated channel is set to the desired print temperature then the screw ensures that the polymer, blends or composites are efficiently melted and mixed prior to extrusion through the nozzle.

Large-scale printers have the added benefit of printing products with a wider range of dimensions than that of FFF.[8] The BAAM printer in Fig. 3 displays the extruder assembly and common configuration for these printers. Like all technologies, BAAM is also subject to some challenges. Since there is such a drastic increase in the print rate, the BAAM printer can struggle to maintain the intended geometry and has decreased surface resolution.[42] The BAAM is also likely to be far more expensive and requires a larger production area.

2.2.2 Selective laser sintering. Parts are formed in SLS by solidifying powder with a laser in a layer-by-layer fashion,[44] building from the bottom up. Unlike E3DP, the feedstock materials for print are stored in a secondary bed that serves as the reservoir. Both beds are held on a piston system to adjust to the required height and a roller sends powder from the reserve to the print area when needed (Fig. 4). One disadvantage of SLS is the resultant rough surface finish. It is recommended that SLS be used when aesthetics and appearance are less crucial. However, this printer is very accurate and would be good for manufacturing large parts. It is important to note that larger parts require more space and this may be a limiting factor for SLS in some cases.[4] The aerospace, biomedical and automotive industries have benefited from the diverse uses of SLS printers to generate parts for aircraft, hearing aids, race cars, and many more structures. However, the materials used are limited for other applications because of the current mechanical properties and lack of reproducibility of parts.[45]

2.3 Methods of optimization prints

Both SLS and E3DP have specific parameters for optimization to print samples based on the printing instructions, sample size and orientation. For FFF/BAAM the major optimized printing parameters include bed temperature, melt temperature, print speed, percent fill, infill type (orientation and pattern), and layer height.[5,47] Parameters often optimized for SLS include laser power, laser scan speed, and particle size of the powder.[48] Further modifications to printed samples can be implemented to optimize the mechanical performance. These post-print treatments include sintering[48] or annealing.[5] This requires holding the samples at elevated temperatures for extended periods of time. However, said processes are time-consuming and require more energy input. Due to the increased time and cost, sintering/annealing is less likely to be implemented in large-scale printing processes. The combination of print optimization can lead to function-specific parts. To systematically optimize prints and observe the influence or dependence of printing parameters, statistical analyses are performed.

2.3.1 Statistical analysis. The design of experiments (DOE) is a method of selecting optimal values or ranges of values, planning and executing a designed plan. Once executed, the

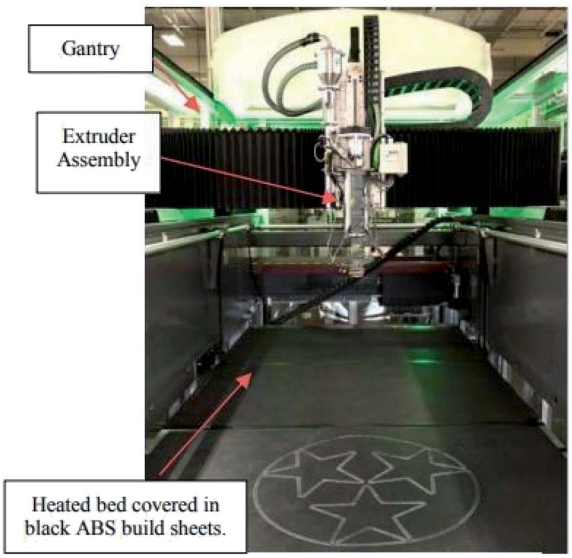

Fig. 3 Big-area-additive-manufacturing extrusion 3D printer.[43] Reprinted with permission from Elsevier: *Procedia Manufacturing*, Copyright 2020, License: 4743161414193.

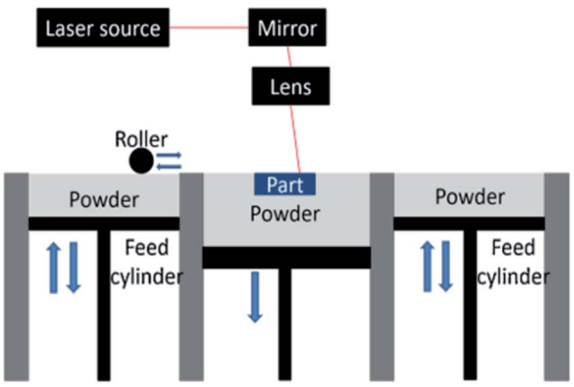

Fig. 4 Selective laser sinter schematic.[46] Reprinted with permission from Elsevier: *Journal of Manufacturing Processes*, Copyright 2020, License: 4743141319375.

collected products are tested, and the obtained results are analyzed. Many works have been completed on DOE with the injection molding of composites[49] and blends[50] to generate novel materials. The same process is now being implemented in 3D printing to generate tailor-made products to serve a wider variety of purposes.

For composites and polymer blends, a mixtures design of experiments can be implemented to optimize samples for a given quality.[49] This method systematically varies the content of each constituent and then analyzes the properties obtained by each combination of materials.[50] This type of DOE focuses on blending,[20] compatibilizing,[17] or making composites.[51] The most common uses for the mixtures design include the following: (1) optimizing the filler/fibre/blending polymer content such that the mechanical properties are maintained or enhanced, (2) replacing the more expensive polymer with a cost-effective replacement (*i.e.*, lower cost filler, polymer).[52]

For 3D printing, the optimization of printing parameters is often of greater importance; more works have focused on using the Taguchi DOE.[53–55] In many cases, parameters such as layer height, print speed and extrusion temperature are correlated to other properties such as dimensional accuracy.[54] These sorts of correlations are important for understanding and implementing in other works such that materials have tailorable mechanical properties or desired aesthetics.

Design of experiments has also been used in 3D printing to optimize the waste generated and the input required to produce samples.[56] One of the most important inputs for optimization is the energy required for the print.[57] However, the input of materials, which is correlated to the cost of the product, can also be optimized.[57] One important difference between energy usage regarding E3DP and SLS arises when SLS requires sintering after printing. This requires additional energy to form the final product. A comparison of the energy consumption for SLS and E3DP could be beneficial when determining the best printing method. The production of parts *via* 3D printing methods has been noted to reduce the cost and production time by 30% and 40% respectively.[58] The major energy consumption for SLS is directly related to the volume and height of the final product.[59] A comparative life cycle assessment (LCA) would be important for comparing the energy consumption as well as waste materials of the SLS and E3DP methods. Further details are highlighted below in Section 6.5. Both the energy consumption and waste have associated costs, which could be reduced if possible to improve the sustainability of the printing processes.[58]

2.4 Optimization and exploration of printing parameters

Often researchers start to test the printability of the materials through a trial-and-error process to generate complete, warpage-free samples. The optimization of printing parameters is not effective unless a range of parameters is known that reduces the warpage (lack of adhesion to bed) and delamination (lack of adhesion between layers). In some cases, only one set of parameters will print after determining the ideal set of parameters.[6] This is referred to as the trial-and-error process.

2.4.1 Finite elemental analysis. Finite elemental analysis (FEA) requires the implementation of computational and analytical practices to model materials and their properties.[60] These models can be used to study fluid dynamics, heat transfer in correlation to the nozzle temperature and dimensional aspects of the printed parts.[60] Many models have been created and analyzed with respect to the kinematics of layer deposition.[61] A FEA can also assist with determining the thermal and mechanical stability of printed samples.[62] Such analysis could be implemented to further reduce the warpage in samples.[63] An extended FEA can also be used to model the fracture behaviour of the samples. This assists in determining which internal printing structure is the most effective for product application.[64] Such analyses are very important when designing prints for mass production.

Finite element analysis has been implemented with 3D printing of the engineering thermoplastic, PEI, to predict the linear elastic behaviour of the printed samples.[65] The FEA software was able to accurately determine Poissons ratio, as well as elastic and shear moduli. This is essential in understanding whether a part can function safely and wholly for the intended purpose. This process can also be used to optimize the 3D printed part based on its design. Space frame and shell analysis are models within the FEA software that analyze the PEI parts containing an internal lattice structure; these methods are cost-effective for optimizing prints.

3. Types of printing materials

This section categorizes the printing materials for both E3DP and SLS. The first type is the neat polymer, which means that the virgin or recycled polymer is printed alone and often requires optimization of processing and printing parameters to generate functional products. The second material type, referred to as blends, is a combination of polymers or polymers and additives, which offer unique property differences as compared to the neat polymer. In some cases, this may include improved dimensional or thermal stability or unique mechanical performances; such aspects are discussed in the sections below. The last category of printing materials is composites. Composites are made from a combination of a distributive phase and a continuous phase. In many cases, composites are formed with fibers or fillers and polymer matrices for unique mechanical performances of printed parts.

3.1 Neat polymers

Although engineering thermoplastics offers superior thermal stability and mechanical performances[4] as compared to commodity thermoplastics, printing can be challenging due to a combination of high melting temperatures, crystallization characteristics and viscoelastic properties.[66] However, there is substantial potential for the use of engineering thermoplastics to address the current limited variability in mechanical properties between commercially available feedstocks. To allow 3D printing to serve a larger variety of applications, there is a demand for

materials that are economically feasible, sustainable and that can fabricate high-quality products each time.

3.2 Blends

Blending polymers is a method for generating diverse feedstock materials for 3D printing applications and can be used to counteract the anisotropic properties that currently limit the performance of many 3D printed products.[67] The use of blending technologies has been used in the injection molding industry with engineering plastics to obtain properties between those of each neat polymer.

For example, engineering thermoplastics have been combined with commodity plastics such as polypropylene (PP),[68] and high-density polyethylene (HDPE).[69] Other combinations with engineering thermoplastics are formed from binary or ternary blends of only engineering thermoplastics such as blending polyesters,[18,70] polycarbonates,[71,72] polyamides,[73,74] ABS,[71,72] and polyether-derived polymers.[75,76] More recently, research has also looked into combining virgin material with recycled material to form the same polymer.[66] The process of SLS produces a lot of waste powder that could be affected by thermal degradation. It has been studied and proven that recycled materials exhibit some differences in mechanical performance as compared to virgin materials. However, blends with these materials could improve the renewability content of the materials and also give new purpose to wastes. As an example, recycled ABS and high-impact polystyrene from electrical components were combined to make value-added products.[77] This diverted waste from potential landfill applications and increased its sustainability *via* a circular economic approach.[78] In addition to increasing the sustainability of printing materials, blending polymers has many other benefits.

The benefits of blending engineering thermoplastics with polymers or polymer-based additives include the following: (1) developing materials with improved mechanical performance, (2) reducing the cost of materials since used materials can be obtained at little to no cost, (3) improving renewable content, and (4) improving the processability of polymers. If these strategies are adopted into 3D printing, there is potential growth for this industry to commercialize new polymer feedstock materials, either blends or composites, for novel printing applications.[67] One of the drawbacks to blending alone relates to the immiscibility of some polymers. Essentially the combined polymers remain as separate and distinctive phases, which could hinder their performance. In this case, further additives are needed to compatibilize and improve the cohesion between the materials. In some cases, the blending materials are chemicals or polymeric materials considered to be additives since they either function as an elastomer as compared to the major system, impact modifier, or compatibilizer. Such materials will be discussed in the additives section below.

3.2.1 Additive materials. Additives, like blending with polymers, are used to tailor the performances such as thermal stability or mechanical properties. Blends with thermoplastic elastomers such as thermoplastic polyurethane (TPU) can help to give a balance of toughness and stiffness.[79] This could be beneficial for applications such as biomedical applications, where there are often the requirements of flexibility and strength. Other important blending materials include compatibilizing agents such as maleic anhydride-grafted polymers and styrene–ethylene–butadiene–styrene (SEBS). Other compatibilizing agents work to improve the miscibility of blended polymers.[7] Compatibilizers and other additives are important to mention since they have the added benefits of (1) diversifying mechanical performance, improving dimensional stability and thermal stability during extrusion, as well as reducing the melt flow index such that it is within a printable range (*i.e.*, near 10 g/10 min [80]). There has been some research with these materials in 3D printing as displayed in Table 1; however, this process was commonly used in extrusion for injection molding in the past. Identified below are also additives that have been implemented in injection molding and may show promise for use in E3DP.

In Table 1, there are also compatibilizing materials that have been implemented in injection molding and may have a purpose in 3D printing. More research is needed to confirm their functionality, economic viability and success.

3.3 Composites

Composites offer benefits in 3D printing, especially E3DP, because the addition of fibre can reduce warpage and the

Table 1 Compatibilizers used in polymer blends and composites

Family	Compatibilizer	Description	Use
Implemented in 3D printing			
Styrene	Styrene–ethylene–butylene–styrene (SEBS)	Thermoplastic elastomer[81]	With ABS[82]
Glycidyl methacrylate (GMA)	Poly(ethylene-*n*-butylene- acrylate-*co*-glycidyl methacrylate) (EBA–GMA)	Impact modifier[6]	EBA–GMA with PTT[6]
	Styrene maleic anhydride (SMA)	Chain extender[6]	SA–GMA with PTT[6]
	Poly(ethylene-*co*-glycidyl methacrylate) (PE-*c*-GMA)	Grafting co-polymer[83]	PE-*c*-GMA with PC[83]
Anhydride	Maleic anhydride (MA)	Coupling agent[7]	SMA with ABS/PA blends[7]
Implemented in injection molding			
Phosphite	Tris(nonylphenyl) phosphite (TNPP)	Stabilizer/crosslinker[84]	TNPP with PA/PLA[84]
Diisocyanate	Polymeric methylene diphenyl diisocyanate (PMDI)	Compatibilizer	[85]

coefficient of thermal expansion.[86] This is a possible solution for generating products that can better serve load-bearing or structural applications such as those in the automotive industry. Since composites have been used extensively in the automotive industry *via* injection molding,[87,88] there is potential for 3D printing to be used for customizable jigs, fixtures, and other assembly parts.[89,90] Composites are also used extensively in the biomedical industry for replacement cartilage products, bones, implants, grafts, screws, and many more.[91] The adaptation of these materials into 3D printing could foster a more personalized approach to medicine, further diversifying the uses of AM technologies.[44,92]

Like injection molding practices, some additives used in 3D printing can be fibres or fillers. Most often, the addition of these materials in both instances serves one or more features including the following: (1) increasing renewability content,[93,94] (2) reduction of the cost by the replacement of expensive polymers with low-cost fillers/fibres,[95,96] (3) acting as a reinforcing agent[97] and improving mechanical properties. Unique composite materials that combine polymer/metal powder are of increasing interest in 3D printing applications.[98] Also, blends of polymers are combined with metal powders to make hybrid materials for 3D printing.[99] The research of these combinations of materials is recent but there are hopes for these materials to serve the biomedical implants industry as well as electrical industry.[99]

4. 3D printing of engineering thermoplastics

4.1 Acrylonitrile butadiene styrene

Acrylonitrile butadiene styrene (ABS) is an engineering thermoplastic derived from a combination of three petroleum sources. The major constituents include acrylonitrile, butadiene and styrene in weight percentages of 15–35, 5–30 and 40–60, respectively.[100] The mixture of these copolymers generates parts that have a balance of rigidity and light-weight traits. The versatility of ABS has made this polymer one of the most popular to use since its development in the 1950s.[100] The polymer has been studied for its use in biomedical applications such as printing handles for scalpels and forceps, as well as other surgical tools.[101] However, this material also functions well in the industrial and electronics sectors. The adaptability of ABS has resulted in its use with various other materials for 3D printing.

4.1.1 Neat ABS in E3DP. The use of ABS in 3D printing was extensively studied in the early 2000s, which has led to much of its use to date.[102,103] Designs of experiments were completed to compare which printing parameters were of the greatest importance in relation to the mechanical performances.[102] These works laid the foundation for the research completed to date.

Since there have been many works completed with ABS in FFF, there has been a shift in focus to printing neat ABS and then adding surface treatments. The surface treatments allow the ABS to be used in areas where it had not been used previously, such as the automotive[104] and medical industries.[105] Traditionally, ABS would not have been used for medical implants as it lacked native biocompatibility as compared to silicones or polyurethanes. However, the lower cost, ease of use and versatility of ABS resulted in efforts to increase its biocompatibility.[105] As a result, the FFF parts from ABS were first sealed *via* submersion in acetone, then treated with poly(-ethylene glycol) methacrylate and subjected to photoinduced graft polymerization. This process enhanced the biocompatibility and hydrophilicity of the samples.[105] Surface modification to ABS then allowed for its potential use in the medical device industry where it had otherwise not been used before. Metalized automotive plastics parts were created through dynamic chemical processing that mixed two substrates to successfully make a conductive film on the outside of non-conductive ABS.[104] This was completed through OH* and super-radical suspensions mixed closely with ABS, followed by the implementation of a titanium dioxide suspension that was subjected to UV irradiation.[104] The successful manufacture of electrically conductive ABS allowed ABS to better serve the automotive industry.[104] Surface modifications to neat ABS have been found to increase the performance and use of FFF products in industries that have not previously used ABS for the described applications.

4.1.2 Neat ABS in SLS. The use and success of printing ABS in SLS required the optimization of the laser power and scanning speed. To further improve the print quality, Chen *et al.*[106] found that pre-heating the powder to 100 °C was beneficial for improved surface finish. To implement ABS in industry, where surface finish is a crucial requirement, the researchers suggested a laser power of 24 W, a scan speed of 2000 mm s^{-1}, and a layer height of 0.2 mm.[106] The printed parts would have the potential for non-structural components of a car, such as dashboards and cup holders, which require a smooth surface finish to maintain the appearance/aesthetics with traditional injection moulded parts. Parameter optimization studies are very helpful in learning what factors impact product quality and production times. These are important aspects to consider when the mass production of a part is required.

4.1.3 ABS blends used in E3DP. One strategy to modify and potentially improve the viscoelastic properties of ABS is to blend with a thermoplastic elastomer. One of the most common thermoplastic elastomers used in FFF is TPU. In one work, ABS was combined with TPU in varying weight concentrations.[79] The prints were generated through a trial-and-error process to determine optimized printing parameters. The printing parameters are described in Table 2. The mechanical performances of the blends are displayed in Table 3. The relative maintenance of mechanical properties was attributed to supramolecular interactions induced by hydrogen bonding between the aromatic and polar groups of ABS and TPU, respectively. Two interesting aspects of this work were as follows: (1) the increased presence of elastomer increased the bond strength of the materials, and (2) the presence of elastomer at the highest studied content of 30 wt% was able to improve the adhesion to the bed and, therefore, result in the ability to print ABS at room temperature.[79] Since ABS material blends can be printed at room temperature, there is no need for

Table 2 Optimal properties for 3D printing engineering thermoplastics

Materials	Method	Parameters	Ref.
ABS/PA 6 and ABS/PA 6/SMA	BAAM	Speed: 1.795 in per s, melting temperature: 220–280 °C	7
ABS	FFF	Melting temperature: 230 °C, speed: 90 mm s^{-1}, bed temperature: 100 °C, layer height: 0.1 mm	
PA		Melting temperature: 260 °C, speed: 72 mm s^{-1}, bed temperature: 80 °C, layer height 0.1 mm	
ABS/PA/SMA		Melting temperature: 245 °C, speed: 30 mm s^{-1}, bed temperature: 80 °C, layer height 0.1 mm	
ABS	FFF	Layer thickness: 0.127–0.3302 mm, raster angle 0°–45°, raster width: 0.2032–0.5588 mm, air gap: −0.00254 to 0.5588 mm, part orientation 0–90°	177
PA 12	FFF	Nozzle: 245 °C, bed temperature: 98 °C, layer height: 0.1 mm, speed: 25 mm s^{-1}, infill density: 75%	168
ABS		Nozzle: 240 °C, bed temperature: 80 °C, layer height: 0.1 mm, speed: 25 mm s^{-1}, infill density: 75%	
Poly(methyl methacrylate) (PMMA)		Nozzle: 240 °C, bed temperature: 90 °C, layer height: 0.1 mm, speed: 25 mm s^{-1}, infill density: 75%	
PEEK		Nozzle: 420 °C, bed temperature: 110 °C, layer height: 0.1 mm, speed: 20 mm s^{-1}, infill density: 75%	
PC		Raster width: 0.432 mm	
PA 12	SLS	Optimized properties for mechanical performance: 0.15 mm layer thickness, feed powder temperature 50 °C, heated platform, 45.7 W fill laser power, 10.9 W outline laser power, 4000 mm s^{-1} speed, 0.3 mm scan spacing Optimized properties for accuracy: 0.10 mm layer thickness, feed powder temperature +100 °C, unheated platform, 11 W fill laser power, 5 W outline laser power, 5000 mm s^{-1} speed, 0.15 mm scan spacing	45
PBT	SLS	Wavelength: 10.6 mm; laser beam diameter: 0.3 mm; laser power for fill and outline: 5, 11, 20 or 30 W; scan speed 5 m s^{-1}; powder bed temperature: 190, 193 °C; layer thickness: 0.1 mm	25
ABS/SEBS 100/0, 95/5, 90/10, 80/20, 50/50	ME3DP	Infill: 100%, layer height: 0.2 mm & 0.27 mm, number of shells: 1, feed rate: 40 mm s^{-1}, travel speed: 55 mm s^{-1}, nozzle diameter: 0.4 mm & 0.8 mm, print temperature 230 °C & 240 °C	12
ABS/UHMWPE/SEBS 75/25/10, 90/10/10	ME3DP	Infill: 100%, layer height: 0.2 mm, number of shells: 1, feed rate: 40 mm s^{-1}, travel speed: 55 mm s^{-1}, nozzle diameter: 0.8 mm, print temperature 230 °C	82
ABS MG47/SEBS-*g*-MA	ME3DP	Nozzle: 230–280 °C, bed temperature: 110 °C, infill density: 100%, print speed: 30 or 60 mm s^{-1}, nozzle diameter: 0.6 mm	
ABS MG94/SEBS-*g*-MA		Nozzle: 230–265 °C, bed temperature: 110 °C, infill density: 100%, print speed: 30 or 60 mm s^{-1}, nozzle diameter: 0.6 mm	
PA/ABS/SMA (85/10.5/4.5)	BAAM (pellets)	Extrudate temperature: 250 °C, print speed: 1.795 inch per s, bead width: 0.289, wall thickness: 0.530 in	7
PA/ABS/SMA 60/40 with 5 to 20 phr of SMA	FFF	Neat ABS: nozzle temperature: 230 °C, layer height: 0.1 mm, bed temperature: 100 °C, print speed: 90 mm s^{-1} Neat PA: nozzle temperature: 260 °C, layer height: 0.1 mm, bed temperature: 80 °C, print speed: 72 mm s^{-1} Compatibilized blends: nozzle temperature: 245 °C, layer height: 0.1 mm, bed temperature: 80 °C, print speed: 30 mm s^{-1}	
ABS/TPU 90/10, 80/20, 70/30	FFF	Nozzle: 230 °C, bed temperature: 110 °C, infill density: 100%, print speed: 30 mm s^{-1}, layer height: 0.2 mm, bed temperature 25 to 90 °C	79
PEK virgin/used: 80/20 & 70/30	SLS	Laser temperature: 368 °C, layer thickness: 0.12 mm, CO_2 laser, exposure time: 12 s, laser power: 15 and 16.5 W, scan speed: 2250 mm s^{-1}	48
PP/PA 6 80/20	SLS	Layer thickness: 100 μm, scan speed: 1257 mm s^{-1}, powder roller: 80 mm s^{-1}, laser power: 6, 7, 8, or 9 W	68
PA 12/HDPE 80/20, 50/50, 20/80	SLS	Laser beam diameter: 250 μm, layer thickness: 150 μm, wavelength 10.6 μm, scan speed: 80 mm s^{-1}, laser power: 3, 6, or 12 W	69

Table 3 Properties of 3D printing engineering thermoplastics, their blends and composites

Sample	Method	Composition (%)	TS (MPa)	TM (GPa)	Strain at break	Ref.
PA 6	BAAM	100	92[a]	5.2[a]	0.022[a]	7
PA/ABS/SMA		85/10.5/4.5	84[a]	3.4[a]	0.032[a]	
PA	FFF	100	42[a]	0.225[a]	2.6[a]	
ABS		100	32[a]	0.320[a]	0.85[a]	
PA 6/ABS/SMA		95 (60/40)/5	52[a]	0.305[a]	0.50[a]	
ABS	FFF	100	10.44–34.61	—	—	177
PA 12	FFF	100	43.08 (1.54)	0.757 (0.194)	—	168
ABS		100	28.97 (0.53)	2.760 (0.050)	—	
Poly(methyl methacrylate) (PMMA)		100	56.25 (1.95)	2.750 (0.050)	—	
PEEK		100	68.04 (7.01)	3.530 (0.010)	—	
PC		100	56[a]	2.01[a]	—	
PA 12	SLS (Lboro)	Used	40	1600	12.5	45
		Virgin	35	1600	4	
	SLS (TNO)	Used	50	1700	17	
		Virgin	50	1700	13	
PBT (LD: laser density (kJ m^{-2}))	SLS	100 (LD: 6.7)	18[a]	1.3 (at 25 °C)	2[a]	25
		100 (LD: 14.7)	55[a]	1.95 (at 25 °C)	3.75[a]	
		100 (LD: 26.7)	51[a]	2.0 (at 25 °C)	3.5[a]	
		100 (LD: 40.0)	42[a]	2.25 (at 25 °C)	3.25[a]	
ABS/SEBS	ME3DP	100 : 0	34.0 (1.74)	—	8.6 (3.3)	12
		95 : 5	25.5 (2.3)	—	3.6 (0.7)	
		90 : 10	26.2 (2.5)	—	4.0 (1.1)	
		80 : 20	25.2 (1.8)	—	11.9 (2.1)	
		50 : 50	18.0 (0.03)	—	47.6 (5.0)	
ABS/UHMWPE/SEBS		75 : 25 : 10	14.7 (0.7)	—	5.7 (0.7)	
		90 : 10 : 10	23.19 (0.8)	—	8.4 (1.0)	
ABS MG47/SEBS-*g*-MA	ME3DP	100 : 0	34.01 (1.3)	2161 (247)	5	82
		75 : 25	17.34 (1.1)	1391 (140)	20	
		50 : 50	12.86 (0.3)	675.7 (151)	30	
		25 : 75	7.33 (0.8)	70.70 (21.3)	500	
ABS MG94/SEBS-*g*-MA	ME3DP	100 : 0	33.04 (2.14)	2280 (341)	5	
		75 : 25	25.09 (1.2)	1484 (141)	9	
		50 : 50	13.21 (0.3)	690.3 (88.4)	65	
		25 : 75	11.55 (0.2)	43.08 (4.46)	850	
		10 : 90	10.16 (0.5)	14.98 (3.69)	1100	
PA/ABS/SMA (*x*-direction)	BAAM (pellets)	85/10.5/4.5	86	3400	3.2	7
PA/ABS/SMA wt%/wt%/phr (*x*-direction)	FFF (filament)	60/40/5	52	300	5	
		60/40/10	16	160	2	
		60/40/20	34	240	2.5	
ABS/TPU	FFF (filament)	Neat ABS	28.5[b]	800	6	79
		90/10	30[b]	830	5	
		80/20	27.5[b]	750	6.5	
		70/30	20.2[b]	725	15	
		Neat TPU	20.5[b]	8	795	
PEK virgin/used blends	SLS (15 W laser power)	100/0	90	—	3.6	48
		80/20	80	—	3.6	
		70/30	75	—	3.0	
PP/PA 12	SLS (6 W laser power)	Neat PP	30	1950	—	68
		Neat PA 12	47	1800	—	
		80/20	10.5	1750	—	
ABS 1,3,5 wt% OMM (*XY* print direction)	FFF	100/0	27.59	1900	1.2	114
		99/1	31.59	2600	1.4	
		97/3	36.33	3000	2.8	
		95/5	39.48	3200	3.6	

[a] Values were approximated from graphical data. [b] Yield strength.

a heated chamber. Chambers are structures that surround the printer and maintain elevated temperatures to reduce the warpage of the samples. The chamber is often maintained at the glass transition temperature of the polymer.[107] There are associated reductions in cost since less energy (electricity) is required to heat and maintain elevated temperatures. Beneficially, the reduced need for a chamber by implementing ABS blends resulted in reductions in the associated cost from energy

consumption. Potentially, the ability to produce ABS blends without a chamber could improve the circular economic aspects of this process by reducing resource consumption. Furthermore, the reduced energy consumption has the potential to slightly reduce the greenhouse gas emissions for each print.

Siqueiros *et al.*[82] also studied the effects of SEBS on two ABS samples of different molecular weights in attempts to develop blends that can function under an array of applications.[82] The mission of this paper was to fabricate new printable materials with a wide variety of physical properties. The blends were optimized through a mixtures design and the chosen parameters are displayed in Table 2. Many successful blends were printed and a wide range of properties were obtained (Table 3). One of the most unique outcomes was that the lower molecular weight ABS (MG94) with 90 wt% SEBS was able to improve the percent elongation at break by 1500% over that of neat ABS.[82] The success of the prints and unique blends demonstrated properties strong enough to support shock absorbers and actuators, which would be a novel application for 3D printed parts.[82] This method was noted to be an economically feasible alternative to thermoplastic elastomer printing materials that are currently on the market.[82]

4.1.4 E3DP of ABS fibre-reinforced composites. Continuous carbon fibre (CF) composites made with thermoplastics are also advantageous for the potential recycling of the materials at the end of their intended life.[86] Thus, the implementation of these materials could improve the sustainability through recycling and could also address concerns about the limited mechanical performance. The continuous fibres showed promise for load-bearing parts[86] that would better serve industries such as automotive and aerospace. The obtained properties are customizable based upon fibre distribution and orientation.[86]

A combination of ABS and CFs was used to synthesize filaments with 10, 20, 30, and 40 wt% CF loading. The CFs and ABS were mixed then placed into a hopper at 220 °C. The print conditions included a nozzle temperature of 205 °C, nozzle diameter 0.5 mm, bed temperature of 85 °C and a layer height of 0.2 mm. Samples of 40 wt% CF could not be printed due to clogging. For the samples that were printed successfully, it was determined that the CFs were often oriented in the flow direction, which was assumed to happen during extrusion. The strength of the composites was also found to increase for the 3D and compression moulded samples with CF showing promising potential for these materials in load-bearing applications.[108] The use of 3D printing parts in load-bearing applications would be an advancement for this technology to serve a greater number of applications.

Additional materials that are often used to fabricate composites include natural fillers or natural fibres. These materials have been used to increase the biocontent or vary the mechanical performances. Osman *et al.*[109] used ABS in combination with rice straw as a method to generate value-added products from waste material. However, this work experienced a decrease in mechanical properties with the addition of natural fibre. Also, the water absorption in the samples increased.[109] Although this work was one of the early uses of natural fillers in 3D printing, more work is required to improve the performances of the materials before implementation on a larger scale.

Sized macadamia nut shells were used as natural filler in compatibilized ABS-based composites for FFF. The matrix contained 3 wt% maleic anhydride and 68 or 78 wt% ABS.[110] Filaments with 1.75 mm diameter were printed with 100% infill through a 0.5 mm nozzle. This work showed promise since the addition of macadamia shells reduced the density of the printed samples in comparison to the other wood fillers used in this study, as well as maintained or enhanced the mechanical performance[110] as compared to other wood-filled materials. The performances of the macadamia composite prints were compared to PLA and ABS-printed samples and found to have lesser mechanical performances. The challenges with some composites, as confirmed in this work, arise from the formation of voids during printing. The voids around the filler reduce the stress dissipation and result in the localized bucking of samples when compressed. Macadamia shells can be obtained at little to no cost since they are a food-industry waste. This means that the nutshells are a by-product of processing the nuts that are then prepared for packaging and consumption. The shell and other remnants left behind are waste biomass. Waste biomass from the food-processing industry is essential for generating sustainable products that align with a circular economy.[111,112] This offers a comparative cost or advantage for mass production.

4.1.5 E3DP of ABS nanocomposites. Nanocomposites in the additive manufacturing industry have attracted increasing interest because the resulting products are often lighter and stiffer than neat polymers alone.[113,114] Lignin-coated cellulose nanocrystals (L-CNC) in combination with ABS were fabricated and studied as a novel material with unique thermal and mechanical properties. Combinations of L-CNC from 0 to 10 wt% were melt-compounded with ABS with a twin-screw extruder at a co-rotating configuration to optimize mixing and dispersion. After filaments were made, samples were printed *via* FFF. One of the critical aspects of this work was the dependency of flow during 3D printing since the temperature of the extrudate impacted the filler mobility and the overall porosity of the samples. Increased porosity in the samples resulted in reduced mechanical performance as compared to injection-molded samples and is one of the limitations with printing nanocomposites.[113]

In work conducted by Weng *et al.*,[114] ABS was combined with organically modified montmorillonite (OMM) and prepared for FFF. Like most 3D printing samples, there was a large decrease in the mechanical properties from the injection-moulded to 3D sample values. The loss in mechanical performance was attributed to a lack of polymer chain entanglement between layers, as well as gaps and voids created by the circular nature of the molten polymer. Interestingly, for this work, the addition of filler was able to increase the tensile strength and modulus as noted in Table 3. Furthermore, the filler was able to decrease the linear coefficient of thermal expansion.[114] This is a beneficial trait as it ensures better dimensional stability at elevated temperatures, *i.e.*, maintaining geometry during printing.

Filaments of ABS and up to 10 wt% multiwalled carbon nanotubes (MWCNT) were generated on a twin-screw extruder and resulted in a filament diameter of 1.7 mm.[115] The 3D printing parameters for these samples were as follows: 0.4 mm nozzle diameter, 30 mm s^{-1} print speed, bed temperature 110 °C, melt temperature of 245 °C and layer thickness of 0.2 mm. The strength was highest in samples with 10 wt% loading. Overall, successful composites were generated.[115] The studied materials were suggested for applications where electrical and thermal conduction were required since the MWCNT increases both these aspects.

4.1.6 SLS of ABS composites. In another work, ABS was used in SLS and was combined with a compatibilizer, impact modifier, thermoplastic starch (30 wt%) and colourant. The preparation of composites required several steps to product filaments. The first step focused on the plasticization of the starch with water and glycerol and compounding (70 °C, 500 rpm). Pelletized starch was then melt-compounded (180 °C, 600 rpm) with ABS, compatibilizer, and impact modifier to generate filaments with the 1.75 mm required diameter for FFF. Samples were successfully printed with a printed melt temperature of 210 °C. It was anticipated that the combination of materials could better serve the industrial, mechanical, electronics and automotive sectors based upon (1) the high thermal stability of the composites, (2) good mechanical properties, and (3) reduced volatile organic compound (VOC) emissions.[116] To validate this experiment and recommend the materials for commercial use, a cost comparison of these materials with existing market products would need to be conducted. This means that if the total cost for raw materials to fabricate these composites is greater than that of the neat polymer (which is commercially available), there needs to be an incentive for industry or the consumer. Essentially, the implementation of new printing materials often requires materials to be economically feasible, viable and sustainable.

4.2 Polyamides

Polyamides (PAs) are formed from condensation reactions between acids and amines. Traditionally, PAs implemented in commercial production were made from petroleum-based resources.[117] However, a push for green chemistry and sustainable product development resulted in some PA polymers now synthesized from biological sources. Examples of biobased sources used to produce PAs include the diacids like succinic acid or sebacic acid. For instance, bio-succinic acid is made from microorganisms where succinic acid is a by-product of their natural Krebs cycle.[118] As for diamines, the counterpart of polyamide synthesis, in some cases is based on organic compounds. An example of this is hexamethylenediamine, which is used in the synthesis of PA 6,6.[119] The relative amounts of diacid and diamine used in the synthesis are the basis for the naming convention of polyamides.[120]

Diversity within the polyamide family of polymers has resulted in polymers that are crystalline, amorphous and fibrous;[119] for this reason, it has been studied extensively.[84,121–123] Polyamides have more recently been studied for use in prosthetics because of the tough, versatile and durable nature of these materials.[92] Some mentionable PAs in this paper include PA 6,6, PA 6, PA 12 and PA 11.

PA 6,6 is formed from a combination of diacids and diamines. It was the first commercialized polyamide and was synthesized at Dupont in 1935.[117] It is formed from the condensation reaction of adipic acid and hexane-1,6-diamine. This material is often used for small fibrous parts such as toothbrush bristles and clothing.[117]

PA 6 was the second polyamide synthesized and became commercially available shortly after PA 6,6.[117] The monomer unit of PA 6, called caprolactam, is a ring-shaped structure that is polymerized by a ring-opening reaction[120] to form the polymer. Each monomer has the chemical formula $C_6H_{11}NO$.

PA 12, an aliphatic engineering thermoplastic, is formed by the ring-opening polymerization or condensation reaction of lauryl lactam or an ω-amino acid, respectively.[124] Uniquely, PA 12 has two stable crystal structures, α- or γ-, where the γ-form is the more stable crystal with a higher melting temperature.[45] The crystalline characteristics are the largest factors that hinder the printability of PA 12.

Polyamide 11 (PA11) is made up of monomer units of 11-aminoundecanoic acid, which is made from castor beans.[125] Not only is this a biologically-based polyamide, but it is very versatile. PA 11 has been used in applications ranging from aerospace to automotive and textiles to sports equipment.[125] Further applications of PA 11 include AM, which is most often implemented in SLS technologies.[125]

4.2.1 E3DP of neat PAs. Polyamides are an exceptionally versatile material that has fostered their use in many industries. Part of the diversity is correlated to the many PA materials available such as PA 12, PA 6, PA 6,6, and many others. One of the unique polyamides studied in E3DP was PA 1012.[126] The success of the print (dimensional stability, completeness and a lack of warpage) was largely influenced by the bed and nozzle temperatures. Other recent works have focused on FFF with PA 12. One of the challenges with PA 12 is that it is semi-crystalline, which can result in more warpage or challenges during printing. It has an optimal nozzle temperature of 250 °C, raster angle of ±45° and 100% infill density, samples with good interlayer bonding and only 4% less ultimate tensile strength than injection molding samples.[126] This work shows great promise for the potential use of PA 12 in commercial and reliable materials for E3DP.

4.2.2 SLS of neat PAs. Although there have been works that have successfully printed PA 12 and PA 11 *via* SLS, there tends to be a lack of reproducibility in parts.[45] A lack of consistency may include reduced dimensional stability or surface appearance,[127] thus, resulting in less consistent products, which may be challenging for mass production where identical parts are important. This may also increase waste since many replicates are required. Often, the lack of reproducibility is a result of the shrinkage of the samples and is largely influenced by the crystal structure. Zarringhalam *et al.*[45] addressed these concerns by taking a closer look at the crystal structure, chemical structure and microstructure of PA 12. The authors found that the γ-form of the crystals was most impacted by the processing conditions.

This work also provided insight into the mechanical performance of PA 12 in SLS; the used powder possessed an increased molecular weight as compared to virgin powder. The increase in the molecular weight of the particle was attributed to better elongation at break properties.[45] Researchers demonstrated that the optimized properties for the SLS process were tailored for the final product based upon mechanical performance or accuracy (Table 3). The optimization of the laser properties for either the accuracy or the mechanical performance was unique for this work since most work is only optimized for one purpose. Other challenges with SLS have been summarized by Schmid *et al.*,[128] who suggest that SLS can be improved through the optimization of (1) particle size and shape; (2) aging, distribution and flowability of the powder; (3) optics and thermal characteristics of the powder, and (4) rheological properties of the bulk material[128] (Fig. 5).

To improve the sustainability of the SLS process, it would be important to reuse the powders that were present during the printing but not sintered. Researchers found that the tensile strength and elongation of samples prepared *via* SLS with used powders were equal, if not better than that of the SLS-printed samples fabricated from virgin polymer.[45] Optical microscopy determined that there were various cores present in the PA 12 samples and this likely affected the mechanical performances (Fig. 6). The more cores present indicated that there was a better melting of the polymer, correlating to better particle fusion and superior mechanical performance. The increased number of crystals, by samples printed on the machine trademarked by the name TNO, likely resulted in the improved mechanical performance.[45] Although the authors only looked at PA, similar trends could likely be found in other polymers. The reuse of materials is both economically and environmentally favourable and should be implemented when possible.

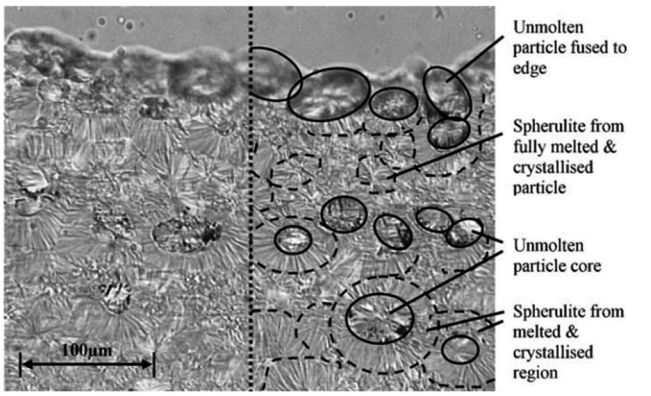

Fig. 6 Optical microscopy image displaying the crystal structure of PA 12.[45] Reprinted with permission from Elsevier: *Materials Science and Engineering: A*, Copyright 2019, License: 4838261169022.

Engineering thermoplastics can also be used to address yet another shortfall of SLS; that is, the thermal degradation of non-sintered powders and their limited re-use. In the long run, if properly addressed and used samples were no longer a waste product, then the use of SLS in mass production could be allowed.[129,130] Since there is an accumulation of aged/used powders in SLS, it is more advantageous to use recycled powder in combination with non-sintered materials to improve cost efficiency and sustainability. To implement used powders, a greater understanding of the chemical and physical effects of aging on the powder's performance and the printed parts is also required. Wudy and Drummer[129] discussed that studying the effects of time and temperature on the thermal properties and molecular characteristics could lead to a solution.[129] Although both the build time and temperature affect the molecular weight, the effect of the chamber temperature on aged samples

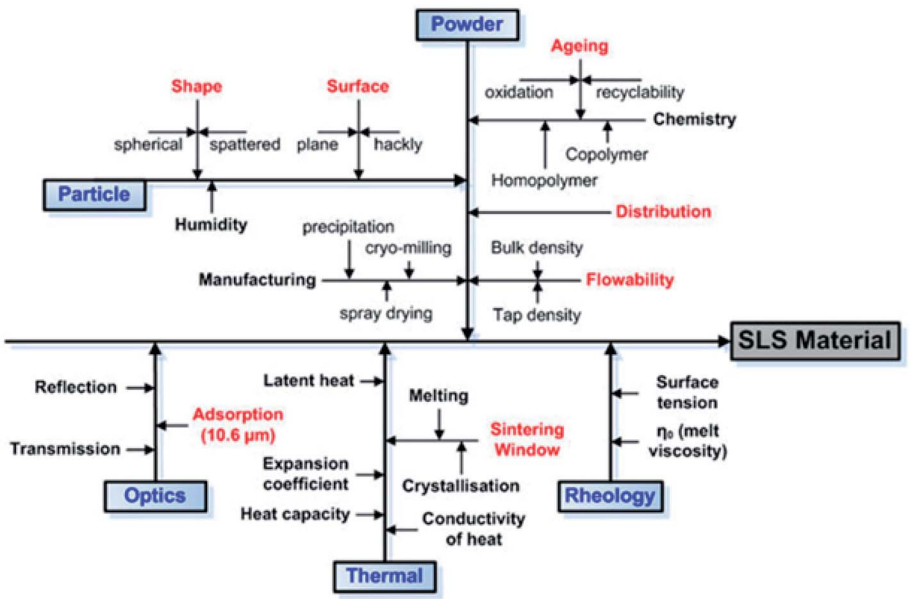

Fig. 5 Parameters of powder and processing conditions that influence SLS printed products.[128] Reprinted with permission from Cambridge University Press: *Journal of Materials Research*, Copyright 2014, License: 4840231185789.

is more substantial. Ultimately, researchers determined that the increased molecular weight results in reduced chain mobility, which is a disadvantage for SLS.[129] This work highlighted the importance of temperature and its correlation with build time based upon the molecular structures present. With a greater understanding of print temperature, build time, molecular structure and their dependence on each other could be taken to industry to further optimize the printing process. This then addresses the shortcomings of SLS, which have prohibited its adaptation to large-scale production to date.

4.2.3 E3DP of PA blends. Polyamide 6 was combined at 30 wt% with a polypropylene (PP) blend. The PP blend was 1.5 : 1 for PP to maleic anhydride grafted poly(ethylene-octene) (MA-*g*-PEO). Therefore, the overall blends were 30 wt% PA and 70 wt% of the 1.5 to 1 blend.[131] Samples were printed at melt temperatures between 220 and 250 °C, bed temperature of 110 °C, 0.1 mm layer height and speed of 30 mm s^{-1}. This material was studied for its shape memory characteristics and reduced warpage with the presence of the compatibilizer, MA-*g*-PEO. Essentially, the compatibilizer fosters improved bonding between the non-polar PP and polar PA 6.[131] If shape memory is a requirement of a printed part, this strategy has the potential to also be applied with other engineering thermoplastics.

4.2.4 Selective laser sintering of PA blends. Used PA powder is described as a powder that has been used in the sintering process but has not been solidified into a part. Used powders often experience thermal degradation and possess reduced properties. As a result, researchers have explored the reuse of PA powder for cost savings benefits.[132] However, to generate viable final products, the layer thickness, laser speed and power, as well as build temperature must be optimized for a desired mechanical performance (such as ultimate tensile strength).[132] The authors determined that the reuse of PA would be possible without compromising the quality of the fabricated part, such as mechanical performance and dimensional accuracy of the print. This further suggests that this material could be used in the biomedical industry to optimize performance, cost and sustainability,[132] where PAs most often are used in prosthetics.[80]

The purpose of this work was to design tailor-made and graded feedstock materials for SLS. Blending is a more cost-effective and industrially implemented strategy to develop novel printing materials as compared to trying to synthesize new polymers.[68] Drummer *et al.*[68] combined polypropylene and PA 12, an immiscible blend, to form samples through varied laser power. This work provided fundamental insight as to how the building temperature can be determined from DSC analysis.[68] Blends of 20 wt% PA 12 and 80 wt% PP were mixed and placed in the bed and printed with the parameters discussed in Table 2. The authors found that the increased laser power resulted in better adhesion between layers as confirmed by microscopic analysis. According to the SEM analysis of the fracture surface, the dispersed phase was noted to have less adhesion to the continuous phase but was also slightly improved through increased laser power. The lack of adhesion between phases was used to explain the reduced mechanical performance of the blends as compared to either neat polymer. Interestingly, the tensile modulus was the only property that remained relatively similar for the blend and neat polymers (Table 3).[68]

Another work combined PA 12 with a more traditional thermoplastic called high-density polyethylene (HDPE).[69] The microcrystalline structures of the blends were measured and compared to the mechanical performances of samples. The printing parameters, noted in Table 2, were optimized to improve the cohesion between materials. The authors determined that the HDPE remained as a co-continuous phase and often remained separated from PA. To improve the laser sintering between materials, the viscosity of HDPE required focus. Overall, the blends could be used as new materials with tailorable properties to improve the applications of SLS.[69]

4.2.5 Polyamide composites in E3DP. Carbon fibre is debatably the most common fibre used with engineering thermoplastics for 3D printing. Many works have been completed with this combination of materials.[108,133,134] Carbon fibre as a reinforcing agent in various polymers for injection molding practices has been of interest due to the enhanced properties as compared to the neat polymer.[135] In hopes of achieving similar improvements to that of injection molding, researchers have combined carbon fibre with PAs for E3DP. Researchers wanted to confirm that the combination of carbon fibre in a PA matrix could improve the impact strength and load capabilities of the printed parts.[136] This paper highlighted a substantial improvement in impact strength based upon the build orientation of the samples, as well as increased impact strength with a greater volume fraction of fibres.[136] This work is important since we are all aware that in most cases, extrusion 3D printed products are affected by anisotropic properties and cannot function well in load-bearing applications. It is important to note the correlation between parameters such as print direction and fibre orientation such that products can be developed with desired mechanical performance and can serve a greater number of applications. Other works with polyamide-based composites have also helped to address the limitations of E3DP such as anisotropic properties and lack of weight-bearing capabilities. Continuous carbon fibres combined with PA 6 were studied based on the optimization of the interface between the fibre and matrix.[137] By sizing the fibres, there was reduced pull-out and improved interfacial adhesion; these materials are more likely to succeed in industrial applications.[137] Another work only required 10 wt% of carbon fibre with PA 12 to result in more than 100% increase in both flexural and tensile strengths.[138] The implementation of carbon fibres is one way to address the limitations in the strength of extrusion 3D printer materials and reduce the impact of anisotropic properties.

Other fibrous materials such as glass fibre and Kevlar have been used in engineering thermoplastics for traditional injection molding. These materials often function in structural components and the fibres act as reinforcing agents to dissipate the load. The same concept is being adapted to 3D printing as mentioned previously. Caminero *et al.*[136] also studied the addition of glass fibres, carbon fibres and Kevlar to PA for FFF. There are two orientations compared for printing such composites which were found to impact their performance. The

first of which is the flat orientation, where the largest face of the impact sample adheres to the bed. The second orientation requires the placement of the sample on-edge, where the surface opposite to the notch is in contact with the bed. All samples were printed with a rectangular infill pattern at 0° and in every case, the samples printed in the on-edge formation resulted in superior performance. The authors offered a partial solution to the limited impact performance of 3D printing samples, which is a short-coming of this technology. The solution is to print samples in the on-edge orientation to orient the fibres to improve the impact properties.[136] Although this is one viable solution to improve the impact strength of the printed parts, there is still a requirement for improved mechanical performances overall. Researchers continue to address these concerns in hopes of developing 3D printing parts with enhanced mechanical performance and improved impact strength.

4.2.6 Selective laser sintering PA composites. In SLS, it is common to combine polyamides with inorganic additives.[139,140] Inorganic additives are those that do not contain carbon, such as silica-based materials, minerals, or metals. Many works also combine fillers derived from petroleum sources such as carbon black or carbon fibre. The combination of fillers helps to fabricate novel materials with varying mechanical,[139] electrical,[139] morphological and thermal properties.[121] This fosters the use of SLS in the automotive, aerospace, thermal,[141] electronics,[121] and energy[139] sectors.

A unique work worth noting is focused on the use of fly ash hollow spheres (FAHS) with PA 12.[141] Fly ash is an inorganic material made from carbonaceous particulate spheres in combination with ash spheres (containing silica). These materials are often generated as a by-product contained in the flue gas from burnt fossil fuels.[142] Polyamide 12 was combined in varying amounts (from 10–25 wt%) with FAHS to make light-weight ceramic foams. These foams can be 3D printed for novel applications. One of the fundamental findings in this work was the reduction in the thermal conductivity of the materials[141] as would be expected when combining a silica-based filler with a polymer. The ceramic foams made in this work could be used to fabricate custom and intricate insulating materials, which suggest that there is potential for this material in high-temperature applications such as automotive and aerospace because of the improved heat transfer. In high-temperature applications, the transfer of heat must be minimized such that there are no changes to the geometric shape or performance of the materials. However, more work is required with FAHS and PA 12 composites to improve the control over the pore size since this directly relates to the strength of the materials.

The combination of PAs with inorganic fillers like carbon black could better serve the electronic industry by fostering the development of electrically conductive materials. Carbon black (CB) was combined at 4 wt% with PA 12 to generate[121] an increase in the electrical conductivity by 5 orders of magnitude as compared to the neat polymer. The mechanical properties of these materials were further refined by the optimization of the laser powder and scanning speed.[121] Although this material is in the preliminary stage of research, it does show promise for electronic applications. This would potentially increase the use of SLS for parts that are traditionally injection-moulded. To further increase the electrical nature of materials, the research has focused on the development, adaptation and success of hybrid materials.

Inorganic additives are used in SLS and other 3D printing methods to diversify the mechanical performances. Diversified mechanical performance, thermal performance or printability may allow 3D printing objects to better serve structural components or other applications where 3D printing is currently not implemented. Hybrid systems can be made from a combination of two or more fillers in one polymer matrix. As an example, $BaTiO_3$ was combined with PA 11 and carbon nanotubes to form a unique nanocomposite material.[139] Samples were printed with 7.5 W laser power, 0.1 mm layer thickness and a laser scanning speed of 7.6m s^{-1}. The combination of filler and polymer showed promise with an increased sintering window and higher laser absorption. These materials resulted in improved dielectric properties and possess the potential to serve a unique purpose in energy storage devices or energy harvesting.[139] This is yet another industry where AM has the potential to benefit from greatly.

4.3 Engineering thermoplastic polyesters

Polyesters are formed from the condensation reaction of an acid, often adipic or sebacic, with an alkanediol.[143] Like PAs, some precursors are now sustainably sourced to improve the biocontent of the polymers.

Polybutylene terephthalate (PBT) is a linear aromatic polyester synthesized from 1,4-butanediol and terephthalic acid. PBT is a versatile engineering thermoplastic with a semi-crystalline structure.[19] Some of the beneficial properties of PBT include excellent electrical properties, good chemical resistance, good processability, and good modulus and strength, even at elevated temperatures.[144] PBT is most commonly used in the automotive sector as a functional material in housing, panels and electrical components.[144]

The synthesis of polyethylene terephthalate (PET) requires the combination of ethylene glycol with terephthalic acid. The exceptional thermal and chemical stabilities of PET have led to its use in automotive applications such as canopy covers.[145] Furthermore, PET is widely used in the beverage and packaging industry but also serves as a material for components in the electrical industry.[146] Other important properties of PET include its resistance to shattering, its relatively light-weight nature, and exceptional barrier properties.[146] The combination of the properties of this semi-crystalline polymer makes it one of the most used engineering thermoplastics to date.

The combination of 1,3-propanediol (PDO) and terephthalic acid is used to synthesize poly(trimethylene terephthalate) (PTT), a high-melting-point polyester.[70] The exceptional thermal stability and elastic recovery have indicated that PTT is suitable for use in engineering and textile applications.[70] Over the last decade, the PDO content of this polymer has been renewably

sourced, resulting in a 37% renewable content as compared to 100% petroleum-based polyesters.[147]

4.3.1 Neat engineering thermoplastic polyesters in E3DP. In addition to improved thermal stability and mechanical performances, improved sustainability content has been important for product development and can be done through the implementation of renewably-sourced or recycled engineering thermoplastics. Recycled polymers often experience a decrease in mechanical performance or changes in other characteristics, such as thermal stability and appearance, as compared to the neat polymer.[24] However, there is a desire to generate products that fulfill aspects of the circular economy, where waste is repurposed for value-added products. The adaptation of used polyester engineering thermoplastics for 3D printing is a promising method to repurpose recycling.

In FFF, Zander *et al.*[66] used recycled PET bottles to generate filament feedstocks. The mechanical performance of the printed samples displayed only a small loss in elongation at break as compared to injection-moulded samples. However, the tensile strength was comparable to other commercially available filaments that are blends of neat PC–ABS.[66] The success of the recycled material was in part attributed to additives that form the PET into bottles prior to the initial use. The additives functioned as nucleating sites that impact crystal growth and size, further improving the printability of the recycled PET. This work provided fundamental insight into how to generate sustainable and diverse filaments to serve a wider range of industrial applications if the material was commercialized.

4.3.2 Neat engineering thermoplastic polyesters in SLS. Historically, injection molding has been used to make consumer goods or products rather than SLS since the samples generally possess superior mechanical performances. However, injection molding is not well suited for circumstances where complex geometries are required, since complex parts often require post-production modifications. It has been suggested in the literature that the use of polyesters like PET has been of interest in SLS because they offer the potential to replace PA 12 (one of the most common commercially used materials).[148]

Poly(butylene terephthalate), commonly used in injection molding, offers high heat resistance and relatively low cost as compared to some engineering thermoplastics.[25] Likewise, PBT also offers good mechanical performance and high chemical resistance,[25] which has led to its adaptation in SLS.[149] Arai *et al.*[149] studied the use of PBT in SLS with careful attention to the printing conditions (Table 2) since the conditions strongly impact the mechanical performance.[25] The milling process of PBT resulted in metal contaminants present in the samples. Beneficially, the metal contaminants acted as nucleating agents (Fig. 7a) to increase the crystallization temperature[25] and mechanical performance (Table 3). Crystallization of the polymer is a fundamental aspect of 3D printing and should be considered prior to printing because it often affects the quality of the print. The addition of the metal contaminants may have been ideal for sample quality but are not ideal where these contaminants could cause a risk during use.[25] Arai *et al.*,[25] were successful at displaying a connection between laser power and mechanical performance. Laser power affected the formation of crystals (Fig. 7b and c). For tensile strength, tensile modulus and elongation at break, the increased laser power resulted in superior performance.[25] Essentially, the industry could prepare tailor-made samples through adjusting the laser power, further allowing the same material to be used in a wide range of applications.

One of the greatest challenges of printing polyesters is that they are crystalline, which creates more defined melting characteristics but results in delamination, warpage/curling as well as limited dimensional stability during the re-crystallization process.[6,150] Such limitations have been investigated for SLS of PET. Bashir *et al.*[150] were able to successfully print the PET powder through the implementation of ideal printing parameters and overcome the limitations mentioned above. The ideal printing parameters with a CO_2 laser included part bed temperature of 225 °C, feed temperature of 160 °C, laser scan speed of 4 m s^{-1} and layer thickness of 100 μm. After printing, the bed plates were left at 200 °C to anneal the samples and beneficially increase the crystallinity. From the process and print optimization, the authors found that PET had a wider processing window, improved part definition, better surface finish, and larger particle size tolerance as compared to PA 12.[150] This was an important discovery for this work as traditionally,

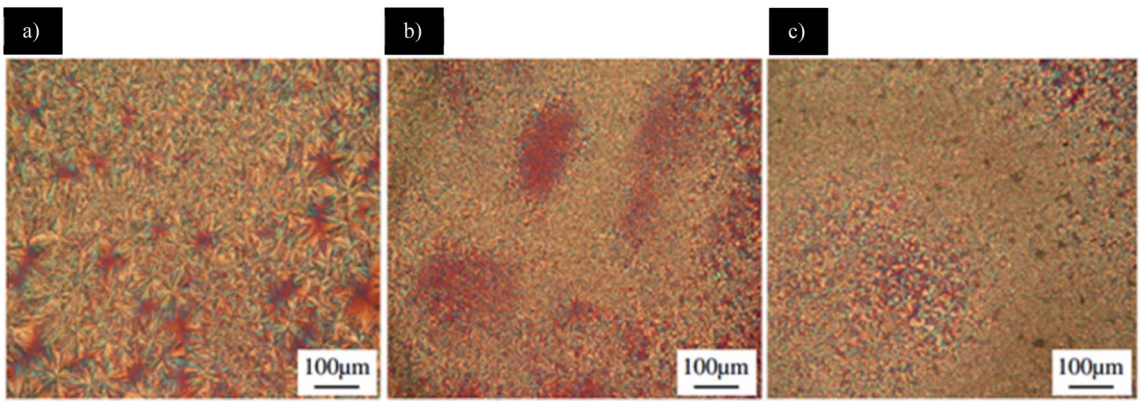

Fig. 7 Polarized optical microscopy images of room temperature (a) pellets, (b) powder, (c) powder with 0.1 wt% silica.[25] Reprinted with permission from Elsevier: *Materials & Design*, Copyright 2019, License: 4694240888567.

PA 12 was the most commonly used material in SLS. The improved part definition is the ability of the printer to maintain the dimensional accuracy of the computer-aided design and a smooth or desired surface finish. Such aspects would make printing this material commercially possible.

4.3.3 Engineering thermoplastic polyester blends for E3DP

Neat polymer with compatibilizer. Polyesters can be challenging to print *via* E3DP based on the crystalline nature of the polymer. To combat this, PTT was combined with a chain extender and an impact modifier for the first time use of PTT in FFF.[6] The additives fulfilled two major criteria that allowed for successful printing. For starters, the additives increased the dimensional stability of the filaments such that they were consistent and met the minimum required thickness. The use of the compatibilizer further reduced the crystallinity, resulting in less warpage during printing. This work shows a method for improving the printability of novel materials through a smooth and easily implemented change during melt extrusion in Fig. 8. This work also highlights the importance of print parameter optimization. Samples were only able to be printed under one set of printing conditions, which were comprised of nozzle temperature at the maximum value of the printer at 290 °C, print layer orientation of 45° and 135° in alternating rows, as well as the use of a brim. The brim is the portion of the printed part outside of the actual sample, which was only deposited in the first layer. The brim is used to improve adhesion to the bed by covering a larger surface area and ensuring consistent flow before printing the part. This strategy is recommended for parts that have trouble adhering to the bed or tend to warp.

4.3.4 Selective laser sintering polyester blends. Blends of PBT, copolymer and flame retardants were combined to make unique blends for SLS of flame-retardant applications. The optimal blends were able to achieve a UL test ration of V0.[149] The use of such materials could foster the growth of SLS technology into other applications where higher flammability performances are required. A cost comparison would be needed to test the economic feasibility of these blends in comparison to existing AM materials.

4.3.5 Engineering thermoplastic polyester composites in E3DP

Fiber-reinforced polyester composites. Biocarbon, also referred to as biochar, is produced from the thermochemical conversion of biobased materials. When heated, biobased materials are converted to carbon-based black material (also referred to here as biocarbon), syngas and bio-oil. In work by Idrees *et al.*,[47] starch-based packing materials were pyrolyzed to generate fillers to combine with recycled PET.[47] All biocarbon was sized to be less than 100 μm, which assists in the reduction of nozzle clogging. Filaments were fabricated with weight loadings from 0.5 to 5%. The tensile modulus was highest for the 5 wt% loaded samples, whereas 0.5 wt% resulted in the greatest strength composites.[47] This suggests that the biocarbon content can be tailored for commercialization, dependent on the functional requirements such as strength modulus or a strength-stiffness balance.

Polyester nanocomposites. Carbon nanotubes (CNT) and PBT filaments were prepared *via* compounding and extruding (240 °C, 50 rpm, 5 min mix time) for FFF by Gnanasekaran *et al.*[37] The authors also combined graphene with other composites to fabricate products that were mechanically stable and electrically conductive. Samples were printed through a 0.4 mm nozzle at 20 mm s^{-1} print speed and nozzle temperature range of 240–260 °C. The CNT biocomposites were found to outperform the graphene composites, however, both materials were successful at producing functional objects at a low fabrication cost.[37] This work also highlights a unique application for 3D printing multi-material products. This was completed with a dual nozzle/head extruder so two materials can be printed simultaneously. For example, the PBT/CNT composites could be printed as one segment of a part, along with neat PLA to make an integrated product.[37] Similar products have been suggested for use in electrical components.[151]

4.3.6 Engineering thermoplastic polyester composites in SLS. The implementation of composites in SLS technologies requires careful attention to fibre orientation as this affects the thermal, mechanical and dimensional accuracy of the materials.[152] A promising study combined PBT with 30 wt% short glass fibre and subjected the samples to single and double scanning motions during the print process. The double scanning practice, depicted in Fig. 9, was able to improve the product quality by reducing the porosity and increasing the mechanical performance.[152] It was suggested that improved mechanical performance, especially in the *z*-direction, was due to reduced resin deterioration. If implementing PBT short glass

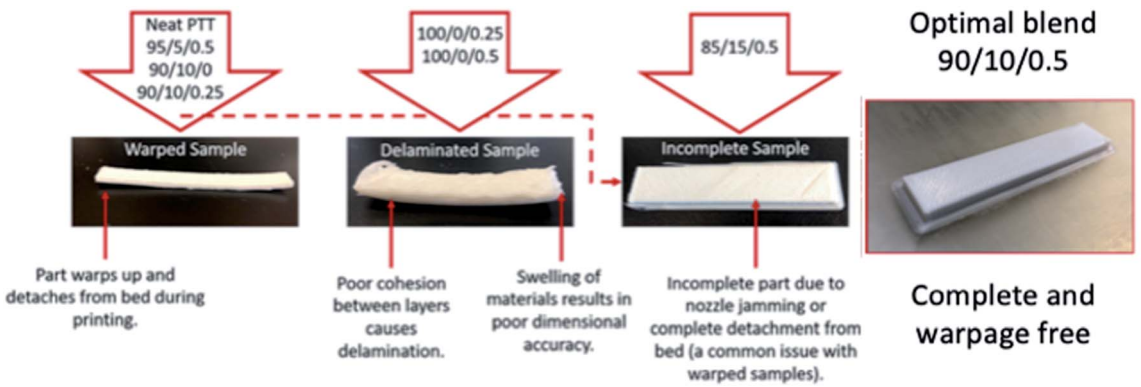

Fig. 8 Optimization of PTT/impact modifier/chain extender blends to make complete samples as novel use for PTT in 3D printing.[6]

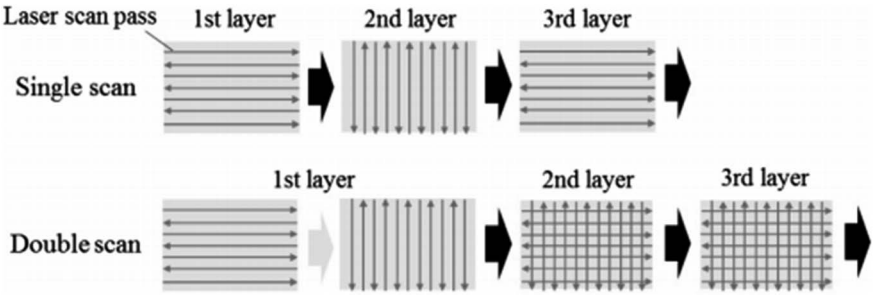

Fig. 9 Single *versus* double scanning for SLS.[152] Reprinted with permission from Elsevier: *Optics and Laser Technology*, Copyright 2019, License number: 4838260880549.

fibre composites commercially, it is recommended to use double scan SLS as well, since there was a slight increase in HDT.[152]

The implementation of this strategy in other composites fabricated *via* SLS may offer commercial viability and enhanced performance to increase the use of SLS parts in various industries.

4.4 Polyether-derived polymers

Polyether-derived polymers are those containing aryl esters and can include polymers like polyetherketone (PEK), polyetheretherketone (PEEK), and polyetherimide (PEI). The structure of the polymers can be found in Fig. 10.

Polyketones are engineering thermoplastics synthesized from a mixture of ketones, aromatic moieties and aryl ethers. This family of polymers is well-known for their exceptional mechanical performance, thermal stability, and resistance to environmental and chemical factors.[13] Another polymer in this family is polyetherimide, which is discussed in greater detail below.

Polyetherimide is an engineering thermoplastic with an amorphous structure, excellent dimensional stability, high heat resistance, good optical properties and reduced flammability.[153] The exceptional properties of this material have led to its use in injection moulded products[154] and more recent use in 3D printing applications.

Polyetherketone was the first polyketone produced and became commercially available in the 1970s through Raychem Corporation. The polymer is semi-crystalline and possesses high impact resistance and natural flame retardation. The synthesis of PEK was not only costly but also produced significant toxic wastes. This resulted in the reduced production of this polymer initially.[13] Since the creation of PEK, the process has been optimized and is now synthesized at a more reasonable cost with reduced environmental concerns. The melting temperature of this polymer is 364 °C,[13] which is much greater than many other engineering thermoplastics and offers a greater advantage for high-temperature applications.

Polyetheretherketone is also a semi-crystalline polymer. Unlike PEK, the synthesis conditions require milder conditions,[13] making this the more sought after polyketone. The melting point of PEEK is 335 °C and the glass transition temperature is 145 °C,[13] suggesting that PEEK may be used instead of PEK for the same applications. The extremely stable nature of PEEK has led to its use in chemical processing applications, aerospace and electrical industries.[13] Also, PEEK has been proven as a useful material for biomedical applications due to its inert nature and biocompatibility.[16] This has been of interest for 3D printing tissue scaffolds and other implants. For example, PEEK has been used to make craniofacial skin tissue scaffolds for personalized medicine.[155]

4.4.1 Neat polyether-derived polymers in E3DP. Wu *et al.*[156] printed neat PEEK and neat ABS as a comparative study. The authors highlighted that both raster angle and layer height affected the mechanical performance of FFF samples. The optimal goal of the paper was to highlight the exceptional properties of PEEK. The tensile, bending and compressive

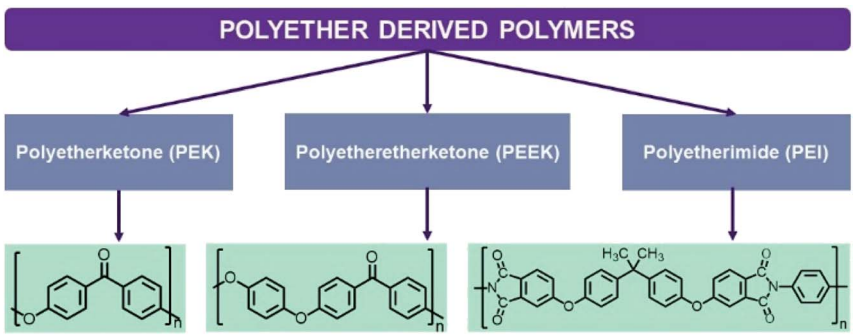

Fig. 10 Chemical structure for PEI, PEK and PEEK which are polyether-based polymers; chemical structures were drawn by the author.

strengths of PEEK were greater than 100% of those of ABS. The use of PEEK may prove to be a promising alternative to ABS for high-strength and high-temperature applications, broadening the overall use of E3DP technology.[156]

The use of PEEK has been more common in FFF than SLS due to challenges with printing since there is such a high melting temperature. In general, PEEK is a relatively expensive polymer that struggles to be penetrated by the laser in SLS.[157] Further challenges with the printing material result from its semi-crystalline nature and high melting temperature.[158] To overcome these challenges, it often requires the use of a custom-built fused filament fabrication printer that reaches higher melting temperatures than standard desktop-sized printers. The materials can be printed for high-temperature applications like automotive and aerospace.[158] In works from Deng *et al.*,[157] the printed samples were tailored for high-impact and high-strength applications. Other works have demonstrated potential in the manufacturing industry for FFF parts.[159] To obtain PEEK parts with the highest tensile strength, it was suggested that they be printed with 100% infill and at an infill direction of $\pm 45^{\circ}$. If PEEK were adapted to the manufacturing industries in FF, modifications would be required since the current strength of cast materials are 1.3 times greater.[159] Methods such as blending, composites, or other additives as outlined in the review could be added to PEEK in FFF to manufacture parts with modifiable properties, which may better serve the automotive, aerospace and electronics industries.

4.4.2 Neat polyether-derived polymers in SLS. The implementation of polyether-derived polymers has been challenging at times due to the high melting temperature. To overcome this, high temperature (HT) SLS machines (HT-SLS) have been fabricated. Such technologies have been used in the aerospace and medical industries to generate highly complex parts.[160] Although the cost of PEEK is comparatively high, the material is of high strength, flame resistance and flexibility, which are very important for 3D technologies to better serve an array of functions[159] such as in the aerospace, electrical and energy sectors.

Materials that are made *via* SLS have the added benefit of not requiring additional tooling costs as compared to the current manufacturing process. Tooling costs are associated with modifications to the product that are required to prepare it for function. This may include removing material or adding further details. The HT-SLS machines have been used to fabricate parts from PEEK.[160] The benefit of using PEEK is that it offers improved mechanical performance as compared to other materials, and performance comparable to injection moulded samples;[160] this suggests that the use of PEEK in SLS may have a better performance than in FFF, since the product performance was similar to those of current market materials. Although the print conditions were not provided in the literature, the use of HT-SLS and the strong mechanical performance of PEEK in SLS have been attributed to the semi-crystalline nature since the final product was 35% crystalline.[160]

4.4.3 Polyether blends in E3DP. Blends of PEI and poly(-ethylene terephthalate)-glycol (PETG) were combined for FFF. At compositions of 5 and 10 wt% PETG, there were improvements in processability but losses in mechanical performance.[161] This research would benefit from the blend optimization through a DOE or a compatibilization study.

4.4.4 Polyether blends in SLS. Poly(ether ketone) was used in combination with a high-temperature laser to produce samples from virgin and recycled polymers. In this work, optimization was essential to develop parts that were less affected by their porosity and had improved surface finish. The optimized parameters are displayed in Table 2. The authors found that particle size greatly impacted the quality of the products. If the powder particles are too large, the product is very porous and has a rougher surface, whereas smaller powders cause poor powder flowability. Poor powder flowability could have resulted in incomplete prints. The optimal size of powder particles was between 75–150 μm.[48] Unique to this work, researchers also looked at the re-ordering between the virgin and used materials during the sintering process. There are two proposed re-ordering mechanisms described in Fig. 11 below. Scenario A was confirmed in this work; in this case, optimized temperatures resulted in a cross-linked site across the entire span of the necking region. This confirmed that the crystalline regions were able to merge and form a strongly sintered part. The potential to re-use materials can be a sustainable and feasible alternative when sintering conditions are optimized, thereby reducing waste and increasing the renewability content of parts. This sort of material valorisation is important for a circular economic approach to sustainable product development. Through parameter optimization in this work, the authors were also able to determine that there were no significant changes in the tensile properties or elongation at break for different laser powers (Table 3).[48] This suggests that a lower laser power of 15 W, rather than 16.5 W, can achieve the same properties at a higher laser power where the increased laser power would consume more energy to operate. Therefore, if used in industry, a lower power laser could save some energy costs and slightly reduce the final cost of the part.

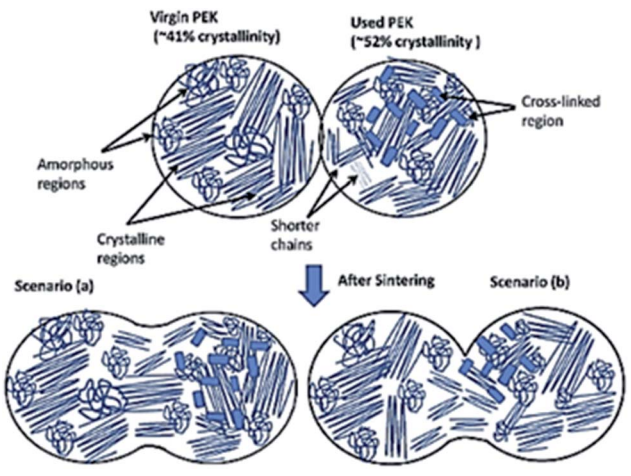

Fig. 11 Two scenarios for re-ordering between virgin and used PEK powders during SLS.[48] Reprinted with permission from Elsevier: *Journal of Materials Processing Technology*, Copyright 2019, License: 4632510363502.

The work by Ghita *et al.*[48] also combined used and virgin PEK to determine how SLS performance is hindered by the porosity of the samples, such that higher porosity leads to stress concentration factors that further enhance the crack propagation within the printed sample. Porous samples perform less favourably and often have a poor surface finish. The concerns for porosity can be addressed as follows: (1) careful material selection to ensure that effective bonding and sintering can occur; (2) optimization of laser power and (3) effective particle size (possibly best between 75–100 μm).[48,162] Surface finish is important not only to avoid defects but also to improve the look of the product. This is also important for SLS in the pharmaceutical industry.[163]

4.4.5 Polyether composites in E3DP. Many of the high-performance engineering thermoplastics are complicated to implement in E3DP due to their high melt viscosity. If the viscosity is too high them there is limited flow from the nozzle. To overcome this challenge; PEEK was combined with inorganic fullerene tungsten sulfide at 2 wt%. The authors suggested that the smooth spherical nature of the filler provided a lubricating effect on the polymer and resulted in reduced melt viscosity. Once viscosity was improved, printed samples exhibited improved mechanical performance and print quality.[164] On gauging the viscosity of the melt flow index, the optimal value was around 10 g min^{-1} for E3DP.[80] Further research is required to assess the cost comparison and environmental impact of the materials. However, the researched materials showed promise with more diverse feedstock for FFF applications.

4.4.6 Polyether composites in SLS. Inorganic compounds have been used in SLS for biomedical applications. Since PEEK is a biocompatible material,[16] it has been adapted for use in tissue scaffolds. Tan *et al.*[165] further added hydroxyapatite to improve the biogenesis and functionality through the controlled pore structure.[165] The laser power and bed temperature were the most important tailored parameters for SLS. When adjusted, the designed scaffolds were produced with desirable characteristics and appearance. The use of PEEK in biomedical applications may foster the growth of personalized medicine.

As compared to commodity plastics, the exceptional performance of PEEK has also indicated its applicability in CF composites to generate materials fit for aerospace.[166] Preliminary works by Yan *et al.*[166] modelled the viscoelastic properties, correlated with temperature, to determine effective printing parameters.[166] The success of the model demonstrated that more work is required to be able to implement these technologies in commercial use.

4.5 Polycarbonate

Polycarbonate (PC) is an engineering thermoplastic derived from carbonic acid and polyhydroxy compounds. It is extremely tough and amorphous with a heat deflection of 130 °C, which is good for many high-temperature applications. It has excellent resistance to scratches and ultra-violet radiation. This polymer also has excellent flame retardant properties.[167]

4.5.1 Neat PC IN E3DP. Research of blends and print optimization is good for generating new feedstock materials. However, if the material is not economically feasible, it cannot be used on a large scale. Cicala *et al.*[168] looked into the use of PC for FFF because it is cheaper to use than PEEK or PLA. This paper would have benefited from providing the printing temperatures of the PC as a comparison to the other data (Table 2). However, the products were successfully printed *via* this process where the maximal strength and modulus were 55 MPa and 2.14 GPa, respectively.[168] In this work and others, alternating layers were printed on raster angles of 30 and 60°. For printing neat PC, it was suggested that these raster angles would achieve the best mechanical properties, therefore, suggesting that there could be the potential for commercialization of this material if feasible.

4.5.2 Neat PC IN SLS. The use of PC in SLS was studied over the last decade to determine the effect of printing parameters on the final printed product.[169] The structural integrity of the printed samples was found to be largely impacted by the size of the powder particles,[169] as well as laser power.[170] Essentially, high laser power is required to improve the strength and density of the materials. If the power is too high, it can result in the degradation of the printed materials, and if the power is too low, it results in samples that are prone to fracturing. In the literature, the optimal laser energy density was 0.1 J mm^{-2} for developing parts with the greatest tensile strength.[170] The improvement in mechanical performance is strongly illustrated *via* the comparison of Fig. 12a and b below. The increased laser power improved the cohesion of particles as noted by reduced voids and a more solid surface. Simple modifications to the printing such as laser power can improve the strength and surface quality of a part. This has led to the success of PC in SLS for commercial or large-scale applications.

4.5.3 PC blends in E3DP. Diversity refers to a larger variability in mechanical performances for printed materials such that they could be used in a greater number of industries, as well as have improved or optimized mechanical performance and dimensional stability. To better fulfill the desire for diversity amongst printing materials, Zhou *et al.*[83] studied the viability of PC and PP blends, as well as their compatibilization. The compatibilizer was made of PE-*c*-GMA with 8 wt% GMA. This work confirms that the addition of compatibilizers increases mechanical performance.[83] The optimal tensile strength was approximately 33 MPa and allowed for greater material diversity. The addition of compatibilizers or other additives has proven that 3D printing can be adapted to other applications that it does not currently operate on.

4.5.4 PC composites in E3DP. As mentioned earlier, there has been significant interest in studying materials made from a combination of metals and polymers. Metals like aluminum have been studied due do the enhanced mechanical performance of printed parts with a lower density and lower cost than other inorganic fillers.[171] Chemical mixing, which occurs during the combination of the metal and the polymer matrix, was found to improve the metallographic, thermal, and mechanical properties through reduced porosity and improved molecular

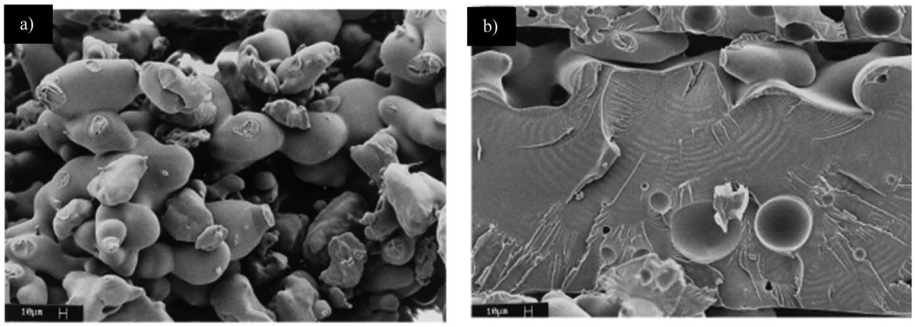

Fig. 12 SLS of PC under (a) 0.036 J mm^{-1} and (b) 0.094 J mm^{-1} laser density, respectively.[170] Reprinted with permission from Elsevier: *Journal of Materials Processing Technology*, Copyright 1999, License number: 4838261399886.

packing.[172] The combination of aluminum (30–60 volume fraction) and PC powders was studied to determine the printability of the materials. Samples were printed *via* FFF while optimizing and correlating resin viscosity, nozzle diameter, volume content of the filler, and its corresponding size.[171] An interesting finding of this work was how clogging occurs during the nozzle flow of composites (Fig. 13). This work displayed that printing PC composites was possible but further work is needed to optimize the printing parameters and reduce the clogging.

4.5.5 PC composites in SLS. Composites from PC in SLS have been studied for some time with some of the older works focusing on inorganic powders like graphite powder with SLS;[173] more recent advances for PC composites involve research for medical applications. Tissue scaffold research has been of interest in the combination of AM and biomedical industries.[33,174] Tissue scaffolds are easily fabricated by SLS since it is a more rapid process than the existing commercial operations.[175] To generate scaffolds that are biocompatible and interactive with the human body, hydroxyapatite (HA) is often added to make composites. Hydroxyapatite is a biocompatible mineral that increases cell adherence. In literature, HA was milled to a very fine powder for many hours before being included at concentrations of 5, 10 and 15 wt% in a PC matrix. The printed materials were optimized and correlations were made between porosity, scan speed, scan spacing, and laser thickness. This study showed that increased porosity and decreased compressive strength were associated with the addition of HA. However, porosity is important for tissue scaffolds since the pores foster the adhesion of cells to the sample.[175] This work highlights important aspects of the implementation of engineering thermoplastic composites for tissue engineering applications.

4.6 Binary and ternary engineering thermoplastic blends

There are blends of multiple engineering thermoplastics that are not able to be classified as solely belonging to a group above. Here, such studies are discussed for the unique mechanical properties that are between both precursor polymers. The blending of engineering thermoplastics is used to generate more diverse feedstock materials that offer a greater range of mechanical properties, variable surface finishes and maintain thermal stability for higher temperature applications. The strategy of blending polymers has been widely studied in injection molding.[21,154,176] Similar processes are being adapted in the additive manufacturing industry to generate tailor-made materials to serve a wider range of applications such as medical, electronics, automotive, electronics and consumer product industries. Many times, blends of engineering thermoplastics also include the use of compatibilizing agents to improve the compatibility of used polymers in the blends. In some cases, the materials may be immiscible and thus hinder mechanical performances.

4.6.1 E3DP of binary and ternary blends. Binary blends are a combination of two polymers; this section will focus on the

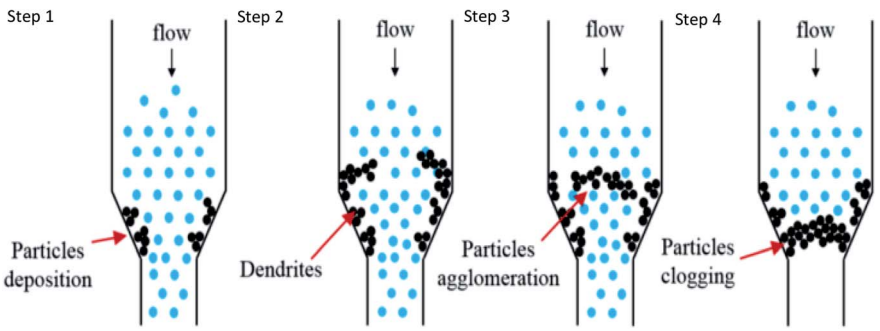

Fig. 13 Modelled clog formation for PC composites *via* FFF.[171] Reprinted with permission from John Wiley and Sons: *Journal of Applied Polymer Science*, Copyright 2019, License: 4732631260702.

binary blends of two engineering thermoplastics. Ternary blends with two engineering thermoplastics and an additional polymer or compatibilizer will also be discussed. The blending of engineering thermoplastics leads to a balance of mechanical and thermal properties. There are also further concerns that can be addressed by blending engineering thermoplastics as discussed below.

In regards to the surface finish, reproducibility and accuracy for FFF printed products, Onwubolu *et al.*[177] determined that printing parameters play a crucial role; optimizing these parameters can tailor the product's aesthetics and mechanical performance. Aesthetics refers to the surface finish and visual quality of the product. Higher quality products maintain dimensional accuracy and are smooth textured visually. The major contributors that affect the mechanical performance and appearance of the product are as follows: part orientation, raster angle, layer thickness, raster width and fill density (referred to as the air gap) (Table 2). Moreover, Onwubolu *et al.*[177] found that the smaller layer thickness of samples resulted in increased tensile strength.[177] Tensile strength was improved through smaller raster widths, negative air gaps, and increased raster angles.[177] However, this strategy may be less favourable for BAAM as more materials are required and the cost of the samples would increase. This work determined that aesthetically pleasing samples with desirable tensile strength and design of experiments were required.

As mentioned above, there are different scales of E3DP that can impact the product performance over the size ranges of industrial-sized machines and home-printing set-ups. Spreeman *et al.*[7] used the term BAAM for industrial printing small-scale platforms FFF for small printers. This work discusses the implementation of engineering thermoplastics blends to generate tailor-made materials with a wider variety of mechanical properties as displayed in Fig. 14c. The printing parameters are summarized in Table 2. To ensure adhesion between constituents and to successfully fabricate blends, a compatibilizing agent is required. Compatibilizing agents improve the cohesion between materials by inducing the cross-linking and branching of polymer chains. The use of polystyrene–maleic-anhydride (SMA) improved the performance of blends of ABS and PA (Table 3). Although this strategy addressed one challenge of FFF, other strategies can be implemented to improve the quality of FFF products.

The mechanical performance of ABS, PA and compatibilized ABS/PA blends that exhibited improved mechanical performances were confirmed by SEM. Under microscopic analyses, samples displayed exceptional layer adhesion (Fig. 14a and b). The BAAM printers produced samples with superior performance with the added benefit of the pellet feed system[7] as noted in Fig. 14c. The compatibilizer used was not only able to function properly but it allowed for two immiscible blends to generate samples with enhanced tensile strength (for SS-FFF systems) as compared to the neat polymer.[7] As suggested by the work of Spreeman *et al.*,[7] the diversity of the pellet-feed systems as compared to the filament feed systems offered a larger variety of printable materials. Moreover, a larger range of printing temperatures also led to improvements in the modulus of the printed samples.

The reasons for the difference in the quality of the products between FFF and BAAM are related to (1) the diversity of the feedstocks, pellets and/or filaments; (2) improved chamber heating, which holds the atmosphere at the desired temperature to reduce warpage;[178] (3) screw extrusion to mix heated polymeric materials more evenly before deposition;[40] (4) improved print resolution.[42]

Rocha *et al.*[12] fabricated binary and ternary polymeric blends of ABS/SEBS and ABS/UHMWPE/SEBS, respectively, where UHMWPE was ultra-high molecular weight polyethylene. The aim of this paper was to discover new compatible blends of materials for FFF to generate greater variability in filament feedstocks to serve a greater number of purposes. The printing parameters were optimized for both the binary and ternary blends and are displayed in Table 2. When adding SEBS to ABS, Rocha *et al.*[12] found a slight decrease in the tensile strength of the ABS/SEBS blends but there was an improvement in the elongation at break (Table 3). The ternary blends experienced

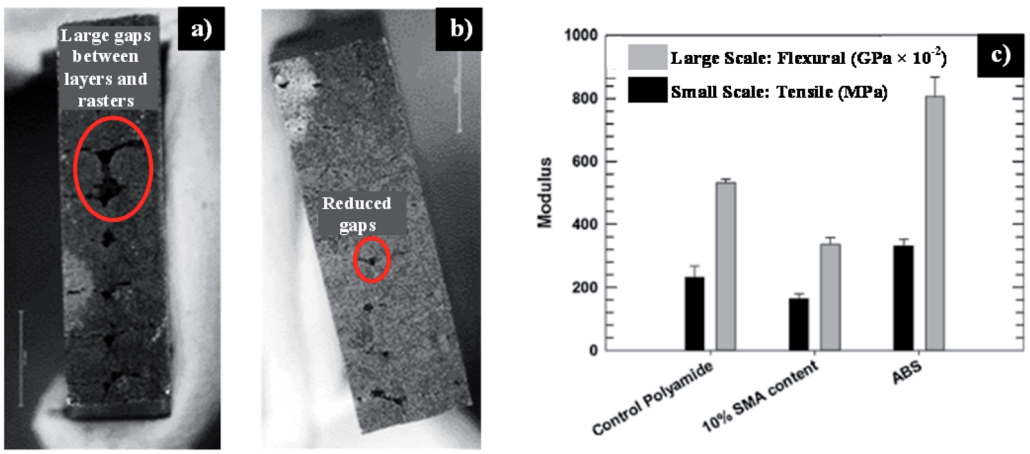

Fig. 14 SEM analysis of the fracture surfaces for BAAM samples (a) PA, (b) PA/ABS compatibilized and (c) a comparison of moduli for small scale *versus* large scale printing.[7] Reprinted with permission from Elsevier: *Additive Manufacturing*, Copyright 2019, License: 4694241403414.

increased tensile strength and elongation at break with increasing UHMWPE content, but the properties were still less than that of the neat ABS polymer. The authors used SEM to explain the decrease in the mechanical properties. The ternary blends had a lack of adhesion between components. Overall, complete and warpage free-samples were printed, which suggested that this material could be further used as a new filament feedstock material with tailorable mechanical performances.[12]

Blends of PC and PEI highlighted an important aspect of 3D printing. To successfully print *via* FFF, the filaments need to be easy to process such that they have a consistent and uniform thickness. The addition of PC (at 5 to 40 wt%) to PEI was able to lower the viscosity, which improved the filament processability. If PC/PEI blends were to be used in FFF the addition of compatibilizers or additives to improve miscibility needs to be studied to avoid phase separation.[179]

Dual polymer filament systems. Rather than blending materials through extrusion to diversify the mechanical properties of printed objects, two distinctive neat polymers can be printed simultaneously through dual extrusion. For toughened parts, ABS has been printed in combination with PC, where a star-shaped internal structure is continuous and encapsulated in ABS. Such material combinations were found to have greater strength as compared to the existing commercially available ABS materials. To further improve the properties of the materials, the prints benefited greatly from annealing. The dual ABS/PC filaments after annealing experienced ductile failure instead of brittle failure like the un-annealed 3D printed samples.[180]

4.6.2 Selective laser sintering of binary and ternary blends. One of the challenges to implementing engineering thermoplastic blends in SLS pertains to the commercial availability of powdered materials.[181] Most often in research, the powder must be made in small batches *via* cryomilling, or is subjected to other size-reducing technologies. If more polymers were commercially available in powder form, it would offer more research potential for all and make the process more time-efficient. This has challenges and would decrease the ability of the materials to be implemented commercially. Dechet *et al.*[181] wanted to study the combination of PBT and PC but there were no powder precursors. The authors then suggested the implementation of a co-grinding process to overcome this limitation. Co-grinding is the process of placing pellets from both polymers into a ball-mill to produce powdered samples. The co-grinding strategy showed promise but does require some further investigation on the resulting chemical and physical nature of each blend.

Polyamide blends have also been investigated *via* SLS with a CO_2 laser. Samples were printed with a 20 W laser, at a scanning speed of 44 mm s^{-1}, chamber temperature of 120 °C, and a layer thickness of 150 μm. PA 12 and PA 6 blends were found to have greater absorption during sintering.[162] One of the key findings in this work was that the porosity and crystalline structures were dependent on the compositions of the samples, rather than the printing conditions. Based on PA 12, the blends were heterogeneous with a mixture of co-continuous and dispersed phases. The success of the printed materials meant that there was a new powder feedstock material that could be used to address concerns such as the limited variability in current materials and diversified mechanical performances.

5. Summary of parameters and materials design to improve 3D printing

To summarize these works and strategies, a point-form list of methods is provided. As noted in Fig. 15, many technical aspects tailor the performance of 3D printed products.

- To improve filament consistency
  - ○ Optimize melt-compounding and extrusion processes[6,37,116]
    - ■ Increase the feed rate
    - ■ Decrease the collection rate of filament
  - ○ Add a compatibilizing agent or impact modifier to increase the molecular weight
- To improve flow during E3DP
  - ○ Blend polymers for unique melt characteristics
  - ○ Optimize nozzle diameter
  - ○ Use BAAM rather than E3DP due to increase melting and mixing before extrusion onto bed[7,178]
  - ○ Modify viscosity[182]
    - ■ Check the melt flow index (MFI). Extremely high or low values will not print;[6,80] MFI values close to 10 g per 10 min print well for FFF[80]
- To reduce warpage or delamination in E3DP
  - ○ Add a brim to the printed sample
  - ○ Change printing parameters like layer height, nozzle temperature
  - ○ Print samples with a bed temperature close to the glass transition temperature
  - ○ Maintain a heated environment during printing: add heated chamber if needed

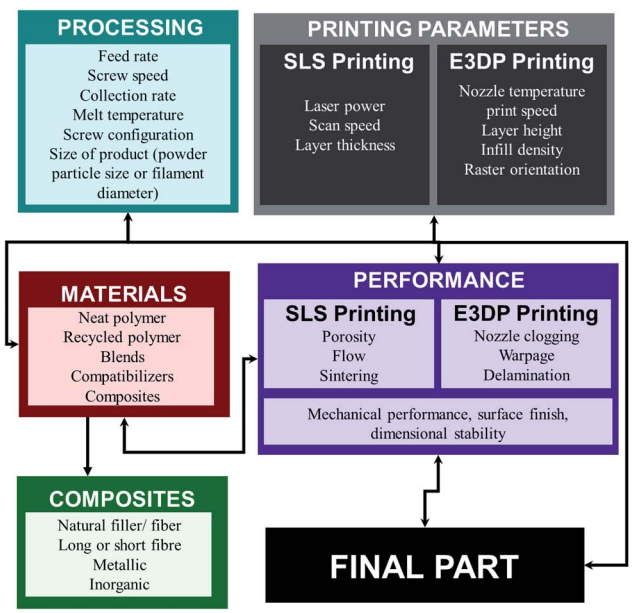

Fig. 15 Interconnectedness of all aspects of printing for product development.

○ Improve the crystallinity of samples[6,183]

■ If a smaller crystal size is desired, add compatibilizer, impact modifier or both

■ If a large crystal size is needed, anneal the parts after printing

• To improve mechanical performance

○ Blend polymers that are miscible or that can form a co-continuous phase[162]

○ Add filler or fibers that have good fiber surface interface

• To improve weight-bearing/impact strength

○ Print long fiber composites with fiber perpendicular to the desired weight direction[136]

• To increase the renewability content

○ In SLS, blend the used and virgin polymers at approximately 20 wt% to maintain the properties but reuse the powders

○ Use biobased polymers like biobased PAs or PTT[6]

○ Fabricate composites with natural/biobased fillers or composites[184]

• To improve thermal and electrical properties

○ Fabricate composites with electrically conductive or thermally conductive materials. For example, fly ash spheres, carbon fibre, graphite[140,141]

○ Blend with flame retardant to improve flame retardancy[149]

• To improve surface finish/print resolution

○ SLS

■ Size the powder between 25–75 μm for reduced porosity

○ E3DP

■ Refine nozzle diameter[185]

• To improve biocompatibility

○ Optimize the surface porosity to improve cell adhesion

○ Use biocompatible polymers like PEEK[155,157,186]

○ Perform surface modifications to traditionally non-biocompatible polymers such as photo-induced graft polymerization[105]

• To improve the filler matrix interface

○ Chemically modify filler surface *via* treatments

○ Add a compatibilizing agent

○ Use polymers, such as PAs, with functional groups, which are more conducive to binding with the filler[187]

6. Feasibility, viability and sustainability

6.1 Economic feasibility

Although many works were completed on engineering thermoplastics, such as ABS, polyamides, PMMA, and PEEK,[168] the implementation of the materials for consumer products is dependent on commercialization and the mass product of research materials. It is well understood that product development is highly impacted by the cost, such that additional costs or high-cost materials must be balanced with exceptional performance or benefits to prove feasible. Some polymers far exceed others in performance, but the cost is too large, such as with PEEK. As an example, PEEK was able to out-perform other engineering thermoplastics by 120% with respect to tensile strength (Table 3).[168] However, this polymer is very expensive and has an extremely high melting temperature,[168] implying that more energy input is required to produce samples. This highlights the current challenge within the 3D printing materials market, where exceptional performance can come with a high cost. Challenges with performance at the expense of the economic viability of 3D printing materials have led researchers to focus on the optimization of printing parameters, polymer blends, or even fabricating composite materials.[2,188,189] Some work may be required to make all engineering thermoplastics cost-competitive.

6.1.1 3D printing in industry. The costs of equipment, labour and resources are important aspects for the industry when adopting 3D printing technologies such as E3DP or SLS as a replacement for other polymer processing methods.[190] A comparison of 3D printing and injection molding has been studied through life cycle costing, which is discussed more below.[191] Other strategies include determining the break-even cost point for each production method *versus* the number of products required. As a reference, Franchetti and Kress compared the injection and FFF processes to find that 187 parts was their break even. If producing less than 187 parts, the equipment, labour and resources are more economically feasible *via* 3D printing.[190] This supports the idea that 3D printing is best used for intricate, complex or custom parts not required in mass-quantities.

6.2 Viability of composites

To date, the addition of fibrous materials has addressed some concerns with a lack of strength and the inability of many 3D printed parts to function in load-bearing applications.[136] In some cases, the improved mechanical properties have been attributed to fibre alignment, uniform particle distribution and layer interactions.[192] However, the adaptation of engineering thermoplastic composites into commercially available printing materials requires the composites to be cost-effective or have superior mechanical performance as compared to the current market options. Not only are there challenges with the materials cost and performance, but some experimental materials are not able to perform successfully due to a lack of interfacial adhesion between the polymer and filler.[192] The lack of adherence between the fibre and the matrix materials is noted by pull-outs defined at point 3 in Fig. 16. Like other 3D printed parts, voids (point 2, Fig. 16) and air bubbles (point 1, Fig. 16) can also be present and reduce the mechanical performance[134] of the composite materials. This is important to understand the potential challenges with printing composites. To overcome this, there is often the need for compatibilizing agents or surface modifications for the filler. This has an associated increase in cost, but would increase the performance of the product.

To date, there are many successful uses of composites implemented in industries to produce viable 3D printed products. Composites produced from FFF or SLS (Table 4) are used in biomedical, electrical, automotive and other industries.[193] Most often, composites are implemented for improved mechanical performances, enhanced electrical characteristics,

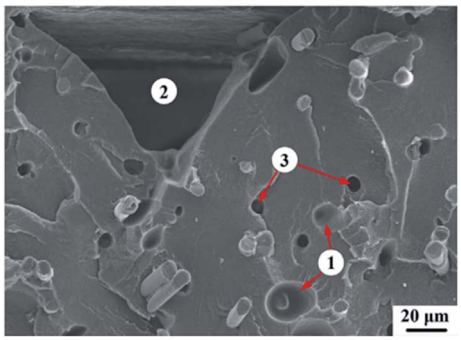

Fig. 16 SEM analysis of the fracture surface of FFF samples.[134] Reprinted with permission from Elsevier: *Composites Part B: Engineering,* Copyright 2019, License: 4694210938408.

increased thermal properties, or better environmental friendliness. The major concept here is that composites can be used to address the limitations mentioned throughout this paper. The distributive phase in composites can dissipate forces more evenly though samples to improve their impact strength.[95,96] If continuous fibres are used, the fibres can be oriented normal to the force and allow 3D printed parts to be used in weight-bearing applications.[136]

6.3 Safety

More recently, there has been significant research interest in the safety hazards associated with SLS and E3DP. For example, the E3DP can result in the release of nanoparticles into the surrounding environment. This is of particular concern for home desktop-sized printers[200] where some of the emitted materials include volatile organic compounds (VOCs) that need to be assessed to ensure safe operation and no long-term health effects.

Recently, 216 VOCs have been attributed to the FFF printing process.[201] In addition to nozzle temperature,[201] emissions are dependent on the filament brand and material.[202] The emissions for PA were 1660 μg per hour as compared to 147 μg per hour for polyvinyl chloride (PVA).[201] When it comes to printing engineering thermoplastics, the common VOCs associated with ABS and PAs are styrene and caprolactam, respectively.[203] Both styrene and caprolactam possess the potential for carcinogenic impacts.[203] Likewise, SLS also produces emissions that need to be studied to determine the potential human health impacts. For SLS of PA 12, the major emissions were carbon dioxide and VOCs.[204] One of the greater concerns with emission in the addition of VOCs is the release of ultra-fine particles.[205] To mitigate some of these concerns, small desktop printers should be operated under fume hoods or well-ventilated areas. This is far easier to implement in industry and research laboratories as compared to home print set-ups. Thus, it is suggested that consumers take special precautions when printing with their desktop printers to reduce health-related concerns. The addition of proper ventilation[205] and personal protective equipment can further reduce the risks associated with printing.

6.4 Sustainability

The success of 3D printing in a great number of industries has given rise to the design and fabrication of materials or parts that are sustainable.[198] Sustainable materials are those that address the societal, environmental and economic aspects of product development, which have reduced impacts on natural resource depletion, reduced emissions[206] and energy consumption.[207] This would help to address concerns about the future environmental impacts of the technology. There are some concerns for 3D printing, which are associated with the accumulation of waste materials, substantial energy consumption and the end of life applicability of equipment and prints. Currently, some 3D printing technologies result in the accumulation of waste materials. Waste is most often generated by FFF/BAAM, due to the required support material that is needed to fabricate the part, but is removed after the print. Some of the prints can also take a long time, which requires greater energy input.[208]

One way to compact the environmental concerns for 3D printing is to generate a design of experiments that focuses on the materials and energy consumption, as well as production and the weight of scrap materials.[56] Reductions in energy consumption and waste can contribute to sustainable longer-term product development.[209]

Less work has been completed with natural fillers or fibres with SLS. This may be due to concerns regarding the degradation of the materials. Most natural fibres have relatively low thermal stability[210] as compared to carbon-based materials. However, biocarbon (also known as biochar) is a sustainable and cost-effective alternative to carbon black.[211] One challenge

Table 4 3D printed composites implemented in industry

Matrix	Filler	Application	General industry	Method	Ref.
ABS	Bakelite–SiC–Al_2O_3	Suggested for automotive	Thermal	FFF	194
PEEK	HA	Scaffolds	Biomedical	SLS	165
ABS	OMMT	Suggested electronics or automotive	Thermal	FFF	114
ABS	Carbon black	Sensors and conductive materials	Electrical	FFF	195
PA 11	Glass beads	Medical clamps and scaffolds	Biomedical	SLS	196
PA 12	CF	Structural parts	Mechanical	SLS	197
PET	Biochar	Automotive parts and engineering applications	Thermal, non-structural	FFF	47
PA 12	Limestone	Manufacturing	Thermal, structural	SLS	198
ABS	Bismuth telluride	Effective energy harvesting materials	Thermoelectric	FFF	199

with the use of natural fibres is the loss in the recyclability of the material at the end of life.[93]

The circular economic approach of 3D printing can be found in Table 4. A reminder that the circular economic approach focuses on recycling, reuse/redistribution, and maintenance, remanufacturing/refurbishing.[212] The other concepts include resource conservation, regeneration and the optimization of processes to increase yields and reduce the leakage of wastes and harmful environmental impacts (Table 5).[213]

6.5 Life cycle assessment

A life cycle assessment (LCA) is used to analyze a product from the development stages to the end of life stage, which includes raw materials extraction, manufacturing of the product, implementation and disposal.[215] This type of analysis is commonly referred to as either cradle-to-cradle (if repurposed) or cradle-to-grave if there is no further use for the product.[216] A completed LCA comparing a computer numerical control (CNC) milling machine to FFF was completed by Faludi *et al.*,[217] where they analyzed the impacts per job in relation to their specific hazards. There were benefits and disadvantages discussed for both processes. For example, for solid parts, the CNC machining produces substantially more waste as compared to FFF processes under maximal utilization. As far as the ecological impacts for each production step, that is manufacturing, electricity consumption waste, transport and disposal, both processes produce the largest impacts during the energy consumption stage during manufacturing. As a result, the largest resulting impacts are on fossil fuel depletion and climate change with respect to human health.[217] From this work, it can be noted that potential reductions in energy consumption for both processes could reduce the environmental impacts of the final products.

To further improve the reliability of LCA, Ma *et al.*[218] suggested that the strategic analysis and design of a sustainability-based LCA could foster the adaptation of AM technologies by both business and industry.[218] The authors suggested that LCA could focus on both an economic assessment as well as consider the social and environmental sustainability of the prints on a case-by-case basis.[218] The processes were broken down into economic, environmental and social considerations. The service and production stages of 3D printed products are the largest emissions producers, impacting climate change, fossil fuel depletion, eutrophication, land use, ozone depletion and others.[218] These impacts have been suggested for consideration by both industry and government, prior to the implementation of AM technologies, as well as a comparison to other technologies like CNC machining as mentioned previously.

There is still some interest focusing in the energy consumption during the 3D printing process in regards to sustainable product development.[115] In understanding the energy consumption of FFF, the global warming impacts can be assessed and used to suggest improvements to the technology. In some cases, reduced energy consumption could reduce operating costs, which also offers an additional benefit to industry.[115] One of the largest energy-consuming steps during printing for FFF is the warming up, where the nozzle is heated to the print temperature. It has been suggested that this be an area of improvement for the printing process.

In addition to printing process modification, a solely economic assessment of AM was proven to be the most important for industries. Such assessments could be implemented when adapting AM technologies to industry. For example, FFF and other AM processes often require limited to no tooling, which reduces energy consumption[219] as compared to processes like CNC machining. There is also less material consumption, which not only saves cost but is less resource demanding and therefore more sustainable.[219]

There have also been some works on LCA of SLS. Researchers have shown that the largest environmental impacts for the process were associated with the waste materials, and subsequent electricity consumption.[59] For E3DP, there are also environmental concerns with waste materials and energy consumption. However, waste materials have been suggested to be reduced based on the optimal parameter selection for a print.[220]

6.6 The future of this technology

For both SLS and E3DP, there is the increasing demand for versatile and sustainable materials. Substantial efforts have been made regarding research into this technology to serve end-use parts, whether automotive parts, medical parts or devices, consumer goods or aerospace.[221] However, two of the greatest challenges for this technology are the commercialization of materials and the scalability of the printing process. As noted

Table 5 Sustainability aspects of 3D printing

Sustainability factor	Description	Ref.
Recycle	The implementation of locally recycled materials for 3D printing without the need for additional transportation or logistics	212
	Recycling of used polymers from one process to the next in SLS printing	48
Maintenance	Repairs for the broken parts of a 3D print can be printed from a device in a faster and cheaper manner	212
Reuse/remanufacture	Redesign parts for 3D printing due to high customizability	212
Manufacturing	Less waste from 3D printing for designs that need no post-printing modifications.	212
	Less transport and logistics to find complex parts since they can be made *via* 3D computer-aided designs and printed	
Resource conservation	The use of natural fillers or other wastes in composite applications since there is valorisation and reduction of waste entering the environment	184 and 214

from the discussed literature, there are many materials with diverse properties to address current industry concerns. However, the feasibility of the materials needs to be studied regarding cost, ease of implementation and materials availability. Other lesser concerns include improving the reproducibility of products, as well as uniformity[222] and dimensional accuracy,[42] and focusing on sustainability[56] and resource (such as time or energy) management.[223] Such considerations seem at this point to be the major set-back for this technology. To address these challenges and concerns, there is a need for further study, as well as possible technology modifications. There are two strategies that may be investigated to improve these processes. The first is process intensification technologies. Process intensification technologies are those that reduce capital investment, reduce raw materials cost and energy use, increase environmental performance and safety, as well as improve quality.[207] The second method for improving this technology is through LCA and interpretation, which was discussed in the paragraphs above.

Some of the challenges experienced through E3DP and SLS may be addressed through the implementation of process intensification technologies.[224] Such technologies may modify the printers structurally or functionally to better address concerns relating to dimensional stability, warpage, delamination, as well as waste and energy consumption.

7. Conclusions

Although engineering thermoplastics are known for their excellent mechanical performances, thermal stability, resiliency and relative chemical inertness over commodify plastics, they do experience some major pitfalls when implemented in additive manufacturing. A general lack of biocompatibility, anisotropy and limited electrical conductivity have halted the progression of 3D printing into more industries. Currently, selective laser sintering and extrusion 3D printing serve a limited number of functions within the automotive, electrical, aerospace and biomedical industries. Strategic materials modification in addition to process and print optimization has evolved polymers, blends and composites to exhibit novel traits to fulfill the desired traits for 3D printed products that are comparable to, or outperform traditional products. Exciting advances have led to the development of 3D printed ceramic foams for automotive applications, electrically conductive customized sensors, surface modified novel biocompatible printing materials, and many more. Each work outline in this review offers vital information on materials, which could diversify the use of E3DP and SLS in industry and boost the growth of AM technologies to unforeseen potential.

List of abbreviations

ABS	Acrylonitrile butadiene styrene
AM	Additive manufacturing
BAAM	Big area additive manufacturing
CNC	Computer numerical control
CF	Carbon fibre
DOE	Design of experiments
E3DP	Extrusion 3D printing
EBA–GMA	Poly(ethylene-*n*-butylene-acrylate-*co*-glycidyl methacrylate)
FDM	Fused deposition modelling
FEA	Finite element analysis
FFF	Fused filament fabrication
GMA	Glycidyl methacrylate
HA	Hydroxyapatite
HDPE	High-density polyethylene
HT-SLS	High-temperature SLS
i.e.	That is
LCA	Life cycle assessment
L-CNC	Lignin-coated cellulose nanocrystals
MA	Maleic anhydride
MWCNT	Multiwalled carbon nanotubes
OMMT	Organic modified montmorillonite
PA	Polyamide
PBT	Poly(butylene terephthalate)
PC	Polycarbonate
PE-*c*-GMA	Poly(ethylene-*co*-glycidyl methacrylate)
PEEK	Polyetheretherketone
PEI	Polyetherimide
PEK	Polyether ketone
PET	Poly(ethylene terephthalate)
PETG	Glycol-modified PET
PHR	Parts per hundred rubber
PI	Polyimide
PLA	Poly(lactic acid)
PMDI	Polymeric methylene diphenyl diisocyanate
PMMA	Poly(methyl methacrylate)
PTT	Poly(trimethylene terephthalate)
SMA	Styrene maleic anhydride
SEBS	Styrene–ethylene–butylene–styrene
SLA	Stereolithography
SLS	Selective laser sintering
SMA	Polystyrene–maleic-anhydride
TNPP	Tris(nonylphenol) phosphite
TPU	Thermoplastic polyurethane
UHNWPE	Ultra-high molecular weight polyethylene
UL	Underwriters laboratory
VOC	Volatile organic compounds
wt%	Weight percent
3D	Three-dimensional

Conflicts of interest

Authors hereby confirm that this manuscript has not been published and is not under consideration elsewhere. Authors declare no conflict of interest.

Acknowledgements

The authors are thankful for the financial support from: (i) the Ontario Research Fund, Research Excellence Program (ORF-

RE09-078) from the Ontario Ministry of Economic Development, Job Creation and Trade, Canada (Project #053970 and 054345); (ii) the Ontario Ministry of Agriculture, Food and Rural Affairs (OMAFRA), Canada University of Guelph, Bioeconomy Industrial Uses Research Program Theme (Project #030252 and 030485); and (iii) the Natural Sciences and Engineering Research Council (NSERC) Canada Discovery Grants Project #400320. This study has also benefited from the facility funding to the Bioproducts Discovery and Development Centre, University of Guelph supported by FedDev Ontario, Canada; OMAFRA Canada; the Canada Foundation for Innovation (CFI); Federal Post-Secondary Institutions Strategic Investment Fund (SIF), Canada; and Bank of Montreal (BMO).

References

1 R. Bogue, *Assem. Autom.*, 2013, **33**, 307–311.
2 A. K. Mohanty, S. Vivekanandhan, J.-M. Pin and M. Misra, *Science*, 2018, **362**, 536–542.
3 T. D. Ngo, A. Kashani, G. Imbalzano, K. T. Q. Q. Nguyen, D. Hui, A. Kashani, G. Imbalzano, K. T. Q. Q. Nguyen, D. Hui, A. Kashani, G. Imbalzano, K. T. Q. Q. Nguyen and D. Hui, *Composites, Part B*, 2018, **143**, 172–196.
4 G. Ryder, B. Ion, G. Green, D. Harrison and B. Wood, *Autom. Constr.*, 2002, **11**, 279–290.
5 C. Benwood, A. Anstey, J. Andrzejewski, M. Misra and A. K. Mohanty, *ACS Omega*, 2018, **3**, 4400–4411.
6 E. V. Diederichs, M. C. Picard, B. P. Chang, M. Misra, D. F. Mielewski and A. K. Mohanty, *ACS Omega*, 2019, 1–11.
7 M. E. Spreeman, H. A. Stretz and M. D. Dadmun, *Addit. Manuf.*, 2019, **27**, 267–277.
8 C. E. Duty, V. Kunc, B. Compton, B. Post, D. Erdman, R. Smith, R. Lind, P. Lloyd and L. Love, *Rapid Prototyp. J.*, 2017, **23**, 181–189.
9 B. G. Compton, B. K. Post, C. E. Duty, L. Love and V. Kunc, *Addit. Manuf.*, 2017, **17**, 77–86.
10 J. Y. Lee, J. An and C. K. Chua, *Appl. Mater. Today*, 2017, **7**, 120–133.
11 R. Melnikova, A. Ehrmann and K. Finsterbusch, *IOP Conf. Ser.: Mater. Sci. Eng.*, 2014, **62**, 012018.
12 C. R. Rocha, A. R. Torrado Perez, D. A. Roberson, C. M. Shemelya, E. MacDonald and R. B. Wicker, *J. Mater. Res.*, 2014, **29**, 1859–1866.
13 G. H. Melton, E. N. Peters and R. K. Arisman, in *Applied Plastics Engineering Handbook: Processing and Materials*, ed. M. Kutz, Elsevier Inc., Waltham, 1st edn, 2011, pp. 7–21.
14 V. R. Sastri, *Engineering Thermoplastics: Acrylics, Polycarbonates, Polyurethanes, Polyacetals, Polyesters, and Polyamides*, Elsevier Inc., 2nd edn, 2013.
15 A. Patil, A. Patel and R. Purohit, *Mater. Today: Proc.*, 2017, **4**, 3807–3815.
16 S. M. Kurtz and J. N. Devine, *Biomaterials*, 2007, **28**, 4845–4869.
17 R. Vadori, M. Misra and A. K. Mohanty, *J. Appl. Polym. Sci.*, 2017, **134**(9), 1–10.
18 A. Asadinezhad, A. Yavari, S. H. Jafari, H. A. Khonakdar, F. Böhme and R. Hässler, *Polym. Bull.*, 2005, **54**, 205–213.
19 N. Dangseeyun, P. Supaphol and M. Nithitanakul, *Polym. Test.*, 2004, **23**, 187–194.
20 M. Zaverl, O. Valerio, M. Misra and A. Mohanty, *J. Appl. Polym. Sci.*, 2015, **132**, 1–11.
21 H. Bai, Y. Zhang, Y. Zhang, X. Zhang and W. Zhou, *J. Appl. Polym. Sci.*, 2006, **101**, 54–62.
22 G. Cicala, G. Ognibene, S. Portuesi, I. Blanco, M. Rapisarda, E. Pergolizzi and G. Recca, *Materials*, 2018, **11**(2), 1–14.
23 B. P. Chang, A. K. Mohanty and M. Misra, *RSC Adv.*, 2018, **8**, 27709–27724.
24 N. E. Zander, M. Gillan, Z. Burckhard and F. Gardea, *Addit. Manuf.*, 2019, **25**, 122–130.
25 S. Arai, S. Tsunoda, R. Kawamura, K. Kuboyama and T. Ougizawa, *Mater. Des.*, 2017, **113**, 214–222.
26 Y. Yuryev, A. K. Mohanty and M. Misra, *RSC Adv.*, 2016, **6**, 105094–105104.
27 A. R. Torrado Perez, D. A. Roberson and R. B. Wicker, *J. Fail. Anal. Prev.*, 2014, **14**, 343–353.
28 J. Torres, M. Cole, A. Owji, Z. DeMastry and A. P. Gordon, *Rapid Prototyp. J.*, 2016, **22**, 387–404.
29 Y. Shao, C. Guizani, P. Grosseau, D. Chaussy and D. Beneventi, *Composites, Part B*, 2018, **149**, 206–215.
30 L. Wang, J. Palmer, M. Tajvidi, D. J. Gardner and Y. Han, *J. Therm. Anal. Calorim.*, 2019, **136**, 1069–1077.
31 M. Kariz, M. Sernek, M. Obućina and M. K. Kuzman, *Mater. Today Commun.*, 2018, **14**, 135–140.
32 Z. C. Kennedy, J. F. Christ, K. A. Evans, B. W. Arey, L. E. Sweet, M. G. Warner, R. L. Erikson and C. A. Barrett, *Nanoscale*, 2017, **9**, 5458–5466.
33 I. Fernández-Cervantes, M. A. Morales, R. Agustín-Serrano, M. Cardenas-García, P. V. Pérez-Luna, B. L. Arroyo-Reyes and A. Maldonado-García, *J. Mater. Sci.*, 2019, **54**, 9478–9496.
34 X. Kuang, D. J. Roach, J. Wu, C. M. Hamel, Z. Ding, T. Wang, M. L. Dunn and H. J. Qi, *Adv. Funct. Mater.*, 2019, **29**, 1–23.
35 F. A. Cruz Sanchez, H. Boudaoud, S. Hoppe and M. Camargo, *Addit. Manuf.*, 2017, **17**, 87–105.
36 G. A. Mazzei Capote, N. M. Rudolph, P. V. Osswald and T. A. Osswald, *Addit. Manuf.*, 2019, **28**, 169–175.
37 K. Gnanasekaran, T. Heijmans, S. van Bennekom, H. Woldhuis, S. de Wijnia and H. Friedrich, *Appl. Mater. Today*, 2017, **9**, 21–28.
38 D. Bourell, D. Espalin, K. Arcaute, D. Rodriguez, F. Medina, M. Posner and R. Wicker, *Rapid Prototyp. J.*, 2010, **16**, 164–173.
39 Y. A. Jin, H. Li, Y. He and J. Z. Fu, *Addit. Manuf.*, 2015, **8**, 142–148.
40 V. Kishore, C. Ajinjeru, A. Nycz, B. Post, J. Lindahl, V. Kunc and C. Duty, *Addit. Manuf.*, 2017, **14**, 7–12.
41 C. Holshouser, C. Newell, S. Palas, C. Duty, L. Love, V. Kunc, R. Lind, P. Lloyd, J. Rowe, R. Dehoff, W. Peter and C. Blue, *Adv. Mater. Processes*, 2013, **171**, 15–17.
42 P. Chesser, B. Post, A. Roschli, C. Carnal, R. Lind, M. Borish and L. Love, *Addit. Manuf.*, 2019, **28**, 445–455.
43 M. Borish, B. K. Post, A. Roschli, P. C. Chesser, L. J. Love, K. T. Gaul, M. Sallas and N. Tsiamis, *Procedia Manuf.*, 2019, **34**, 482–488.

44 F. Fina, A. Goyanes, S. Gaisford and A. W. Basit, *Int. J. Pharm.*, 2017, **529**, 285–293.
45 H. Zarringhalam, N. Hopkinson, N. F. Kamperman and J. J. de Vlieger, *Mater. Sci. Eng., A*, 2006, **435–436**, 172–180.
46 Z. Xu, Y. Wang, D. Wu, K. P. Ananth and J. Bai, *J. Manuf. Process.*, 2019, **47**, 419–426.
47 M. Idrees, S. Jeelani and V. Rangari, *ACS Sustainable Chem. Eng.*, 2018, **6**, 13940–13948.
48 O. R. Ghita, E. James, R. Trimble and K. E. Evans, *J. Mater. Process. Technol.*, 2014, **214**, 969–978.
49 N. Zarrinbakhsh, A. K. Mohanty and M. Misra, *Composites, Part A*, 2019, **119**, 246–260.
50 O. Valerio, M. Misra and A. K. Mohanty, *Polym. Test.*, 2018, **65**, 420–428.
51 A. Gowman, A. Rodriguez-Uribe, F. Defersha, A. K. Mohanty and M. Misra, *J. Appl. Sci.*, 2020, **137**, e49061.
52 N. Zarrinbakhsh, F. M. Defersha, A. K. Mohanty and M. Misra, *J. Appl. Polym. Sci.*, 2014, **131**(13), 1–11.
53 S. Mahmood, A. J. Qureshi and D. Talamona, *Addit. Manuf.*, 2018, **21**, 183–190.
54 A. Alafaghani and A. Qattawi, *J. Manuf. Process.*, 2018, **36**, 164–174.
55 M. Vishwas, C. K. Basavaraj and M. Vinyas, *Mater. Today: Proc.*, 2018, **5**, 7106–7114.
56 C. A. Griffiths, J. Howarth, G. De Almeida-Rowbotham, A. Rees and R. Kerton, *J. Cleaner Prod.*, 2016, **139**, 74–85.
57 F. Ma, H. Zhang, K. K. B. Hon and Q. Gong, *J. Cleaner Prod.*, 2018, **199**, 529–537.
58 T. Peng, *Procedia CIRP*, 2016, **40**, 62–67.
59 K. Kellens, R. Renaldi, W. Dewulf, J. P. Kruth and J. R. Duflou, *Rapid Prototyp. J.*, 2014, **20**, 459–470.
60 H. Xia, J. Lu and G. Tryggvason, *Rapid Prototyp. J.*, 2018, **24**, 973–987.
61 J. F. Agassant, F. Pigeonneau, L. Sardo and M. Vincent, *Addit. Manuf.*, 2019, **29**, 100794.
62 A. Cattenone, S. Morganti, G. Alaimo and F. Auricchio, *J. Manuf. Sci. Eng.*, 2019, **141**, 1–17.
63 A. Ahmadi Dastjerdi, M. R. Movahhedy and J. Akbari, *Addit. Manuf.*, 2017, **18**, 285–294.
64 R. Ghandriz, K. Hart and J. Li, *Addit. Manuf.*, 2020, **31**, 100945.
65 S. Bhandari and R. Lopez-Anido, *Addit. Manuf.*, 2018, **22**, 187–196.
66 N. E. Zander, M. Gillan and R. H. Lambeth, *Addit. Manuf.*, 2018, **21**, 174–182.
67 D. Roberson, C. M. Shemelya, E. MacDonald and R. Wicker, *Rapid Prototyp. J.*, 2015, **21**, 137–143.
68 D. Drummer, K. Wudy, F. Kühnlein and M. Drexler, *Phys. Procedia*, 2012, **39**, 509–517.
69 G. V Salmoria, J. L. Leite, C. H. Ahrens, A. Lago and A. T. N. Pires, *Polym. Test.*, 2007, **26**, 361–368.
70 G. Li, K. Wang, S. Li and Y. Shi, *J. Macromol. Sci., Part B: Phys.*, 2007, **46**, 569–580.
71 S. Bärwinkel, A. Seidel, S. Hobeika, R. Hufen, M. Mörl and V. Altstädt, *Materials*, 2016, **9**(8), 659.
72 B. S. Lombardo, H. Keskkula and D. R. Paul, *J. Appl. Polym. Sci.*, 1994, **54**, 1697–1720.
73 G. Serpe, J. Jarrin and F. Dawans, *Polym. Eng. Sci.*, 1990, **30**, 553–565.
74 C. S. Moran, A. Barthelon, A. Pearsall, V. Mittal and J. R. Dorgan, *J. Appl. Polym. Sci.*, 2016, 1–9.
75 G. Crevecoeur and G. Groeninckx, *Macromolecules*, 1991, **24**, 1190–1195.
76 A. Arzak, J. I. Eguiazábal and J. Nazábal, *J. Appl. Polym. Sci.*, 1997, **65**, 1503–1510.
77 D. Hirayama and C. Saron, *Polymer*, 2018, **135**, 271–278.
78 Ellen Macarthur Foundation, *What is a Circular Economy?*, https://www.ellenmacarthurfoundation.org/circular-economy/what-is-the-circular-economy?gclid=CjwKCAjwgdX4BRB_EiwAg8O8Hbf1VIMqge2f3KS482kVravEYIXKlF76UAJPLyyykjrMwgp9PnIXJRoCPIIQAvD_BwE, accessed 28 March 2019.
79 A. S. De León, A. Dominguez-Calvo and S. I. Molina, *Mater. Des.*, 2019, **182**, 108044.
80 S. Wang, L. Capoen, D. R. D'hooge and L. Cardon, *Plast., Rubber Compos.*, 2018, **47**, 9–16.
81 N. S. Allen, M. Edge, A. Wilkinson, C. M. Liauw, D. Mourelatou, J. Barrio and M. A. Martínez-Zaporta, *Polym. Degrad. Stab.*, 2001, **71**, 113–122.
82 J. G. Siqueiros, K. Schnittker and D. A. Roberson, *Virtual Phys. Prototyp.*, 2016, **11**, 123–131.
83 Y. G. Zhou, B. Su and L. S. Turng, *Rapid Prototyp. J.*, 2017, **23**, 869–880.
84 J. I. Gug, J. Soule, B. Tan and M. J. Sobkowicz, *Polym. Degrad. Stab.*, 2018, **153**, 118–129.
85 S. Sahoo, M. Misra and A. K. Mohanty, *J. Appl. Polym. Sci.*, 2013, **127**, 4110–4121.
86 L. G. Blok, M. L. Longana, H. Yu and B. K. S. Woods, *Addit. Manuf.*, 2018, **22**, 176–186.
87 O. Akampumuza, P. M. Wambua, A. Ahmed, W. Li and X. Qin, *Polym. Compos.*, 2017, **38**, 2553–2569.
88 P. Abel, T. Gries and T. Troester, in *Fatigue of Textile Composites*, ed. V. Carvelli and S. V. Lomov, Woodhead Publishing, 2016, pp. 383–401.
89 G. Dwivedi, S. K. Srivastava and R. K. Srivastava, *Int. J. Phys. Distrib. Logist. Manag.*, 2017, **47**, 972–991.
90 G. Schuh, G. Bergweiler, F. Fiedler, K. Lichtenth and S. Leimbrink, *Proc. 2019 IEEE IEEM*, 2019, pp. 484–488.
91 J. Chen, W. Shi, A. J. Norman and P. Ilavarasan, *IEEE Int. Symp. Electromagn. Compat.*, 2002, **2**, 861–865.
92 J. ten Kate, G. Smit and P. Breedveld, *Disabil. Rehabil.: Assist. Technol.*, 2017, **12**, 300–314.
93 A. C. Gowman, M. C. Picard, L. Lim, M. Misra and A. K. Mohanty, *BioResources*, 2019, **14**(4), 1–46.
94 S. Muniyasamy, M. M. Reddy, M. Misra and A. Mohanty, *Ind. Crops Prod.*, 2013, **43**, 812–819.
95 M. C. Picard, A. Rodriguez-Uribe, M. Thimmanagari, M. Misra and A. K. Mohanty, *Waste Biomass Valorization*, 2020, **11**, 3775–3787.
96 A. Gowman, T. Wang, A. Rodriguez-Uribe, A. K. Mohanty and M. Misra, *ACS Omega*, 2018, **3**, 15205–15216.
97 X. Tian, T. Liu, C. Yang, Q. Wang and D. Li, *Composites, Part A*, 2016, **88**, 198–205.

98 R. Matsuzaki, T. Kanatani and A. Todoroki, *Addit. Manuf.*, 2019, **29**, 100812.
99 Y.-H. Chueh, C. Wei, X. Zhang and L. Li, *Addit. Manuf.*, 2020, **31**, 100928.
100 L. Mckeen, in *Fatigue and Tribological Properties of Plastics and Elastomers*, William Andrew Applied Science Publishers, 2nd edn, 2010, pp. 51–71.
101 J. Y. Wong and A. C. Pfahnl, *Aviat., Space Environ. Med.*, 2014, **85**, 758–763.
102 S. H. Ahn, M. Montero, D. Odell, S. Roundy and P. K. Wright, *Rapid Prototyp. J.*, 2002, **8**, 248–257.
103 J. F. Rodriquez, J. P. Thomas and J. E. Renaud, *Rapid Prototyp. J.*, 2001, **7**, 148–158.
104 L. Magallón-Cacho, J. J. Pérez-Bueno, Y. Meas-Vong, G. Stremsdoerfer and F. J. Espinoza-Beltrán, *Surf. Coat. Technol.*, 2011, **206**, 1410–1415.
105 E. J. McCullough and V. K. Yadavalli, *J. Mater. Process. Technol.*, 2013, **213**, 947–954.
106 Q. G. Chen and J. C. Zhang, in *Advanced Manufacturing Technology, ADME 2011*, Trans Tech Publications Ltd, 2011, vol. 314, pp. 738–741.
107 K. G. J. Christiyan, U. Chandrasekhar and K. Venkateswarlu, *IOP Conf. Ser.: Mater. Sci. Eng.*, 2016, **114**, 012109.
108 H. L. Tekinalp, V. Kunc, G. M. Velez-Garcia, C. E. Duty, L. J. Love, A. K. Naskar, C. A. Blue and S. Ozcan, *Compos. Sci. Technol.*, 2014, **105**, 144–150.
109 M. A. Osman and M. R. A. Atia, *Rapid Prototyp. J.*, 2018, **24**, 1067–1075.
110 J. Girdis, L. Gaudion, G. Proust, S. Löschke and A. Dong, *JOM*, 2017, **69**, 575–579.
111 M. Picard, S. Thukur, M. Misra, D. F. Mielewski and A. K. Mohanty, *Sci. Rep.*, 2020, **10**, 3310.
112 Z. Li, C. Reimer, M. C. Picard, M. Misra and A. K. Mohanty, *Front. Mater.*, 2020, **7**(3), 1–12.
113 X. Feng, Z. Yang, S. S. H. Rostom, M. Dadmun, Y. Xie and S. Wang, *J. Appl. Polym. Sci.*, 2017, **134**, 1–8.
114 Z. Weng, J. Wang, T. Senthil and L. Wu, *Mater. Des.*, 2016, **102**, 276–283.
115 V. A. Balogun and B. I. Oladapo, *Int. J. Eng., Trans. A*, 2016, **29**, 1034–1041.
116 C. C. Kuo, L. C. Liu, W. F. Teng, H. Y. Chang, F. M. Chien, S. J. Liao, W. F. Kuo and C. M. Chen, *Composites, Part B*, 2015, **86**, 36–39.
117 V. R. Sastri, in *Plastics in Medical Devices: Properties, Requirements, and Application*, Elsevier Inc., Burlington, 2nd edn, 2013, pp. 161–170.
118 J. J. Beauprez, M. De Mey and W. K. Soetaert, *Process Biochem.*, 2010, **45**, 1103–1114.
119 J. A. Brydson, in *Plastics Materials*, Butterworth-Heinemann, Oxford, 7th edn, 1999, pp. 478–530.
120 L. McKeen, in *Plastic Films in Food Packaging: Materials, Technology and Applications*, ed. S. Ebnesajjad, Elsevier Inc., 2012, pp. 1–15.
121 S. R. Athreya, K. Kalaitzidou and S. Das, *Mater. Sci. Eng., A*, 2010, **527**, 2637–2642.
122 H. Zhang, S. Li, C. J. Branford White, X. Ning, H. Nie and L. Zhu, *Electrochim. Acta*, 2009, **54**, 5739–5745.
123 A. Codou, M. Misra and A. K. Mohanty, *Composites, Part A*, 2018, **112**, 1–10.
124 W. Griehl and D. Ruesteivi, *Ind. Eng. Chem.*, 1970, **62**, 16–22.
125 B. Herzog, M. I. Kohan, S. A. Mestemacher, R. U. Pagilagan and K. Redmond, *Ullmann's Encycl. Ind. Chem.*, 2013, 1–36.
126 H. Li, S. Zhang, Z. Yi, J. Li, A. Sun, J. Guo and G. Xu, *Rapid Prototyp. J.*, 2017, **23**, 973–982.
127 S. C. Ligon, R. Liska, J. Stampfl, M. Gurr and R. Mülhaupt, *Chem. Rev.*, 2017, **117**, 10212–10290.
128 M. Schmid, A. Amado and K. Wegener, *J. Mater. Res.*, 2014, **29**, 1824–1832.
129 K. Wudy and D. Drummer, *Addit. Manuf.*, 2019, **25**, 1–9.
130 P. Obst, M. Launhardt, D. Drummer, P. V. Osswald and T. A. Osswald, *Addit. Manuf.*, 2018, **21**, 619–627.
131 X. Peng, H. He, Y. Jia, H. Liu, Y. Geng, B. Huang and C. Luo, *J. Mater. Sci.*, 2019, **54**, 9235–9246.
132 K. Kozlovsky, J. Schiltz, T. Kreider, M. Kumar and S. Schmid, *Procedia Manuf.*, 2018, **26**, 826–833.
133 W. Ye, G. Lin, W. Wu, P. Geng, X. Hu, Z. Gao and J. Zhao, *Composites, Part A*, 2019, **121**, 457–464.
134 F. Ning, W. Cong, J. Qiu, J. Wei and S. Wang, *Composites, Part B*, 2015, **80**, 369–378.
135 D. D. L. Chung, *Carbon Fiber Composites*, Butterworth-Heinemann, Elsevier, BS Publications, Newton, 1994.
136 M. A. Caminero, J. M. Chacón, I. García-Moreno and G. P. Rodríguez, *Composites, Part B*, 2018, **148**, 93–103.
137 T. Liu, X. Tian, M. Zhang, D. Abliz, D. Li and G. Ziegmann, *Composites, Part A*, 2018, **114**, 368–376.
138 G. Liao, Z. Li, Y. Cheng, D. Xu, D. Zhu, S. Jiang, J. Guo, X. Chen, G. Xu and Y. Zhu, *Mater. Des.*, 2018, **139**, 283–292.
139 F. Qi, N. Chen and Q. Wang, *Mater. Des.*, 2018, **143**, 72–80.
140 A. Jansson and L. Pejryd, *Addit. Manuf.*, 2016, **9**, 7–13.
141 M. Li, A. N. Chen, X. Lin, J. M. Wu, S. Chen, L. J. Cheng, Y. Chen, S. F. Wen, C. H. Li and Y. S. Shi, *Ceram. Int.*, 2019, **45**, 20803–20809.
142 N. L. Rose, E. Change, B. Way, L. Uk and W. Oap, *Environ. Pollut.*, 1996, **91**(2), 245–252.
143 M. Sokolsky-Papkov, R. Langer and A. J. Domb, *Polym. Adv. Technol.*, 2013, **22**(5), 502–511.
144 C. V. Pious and S. Thomas, in *Printing on Polymers*, eds. J. Izdebska and S. Thomas, William Andrew Publishing, 2016, pp. 21–39.
145 G. Karthik, K. V Balaji, R. Venkateshwara and B. Rahul, in *SAE Technical Paper*, SAE International, 2015, pp. 1–4.
146 C. B. Crawford and B. Quinn, in *Microplastic Pollutants*, ed. C. B. Crawford and B. Quinn, Elsevier, 2017, pp. 57–100.
147 J. V. Kurian, in *Natural fibers, Biopolymers, and Biocomposites*, ed. A. K. Mohanty, M. Misra and L. T. Drzal, Taylor & Francis, 2005, pp. 503–530.
148 H. Gu, Z. Bashir and L. Yang, *Addit. Manuf.*, 2019, **28**, 194–204.
149 S. Arai, S. Tsunoda, A. Yamaguchi and T. Ougizawa, *Opt. Laser Technol.*, 2019, **117**, 94–104.

150 Z. Bashir, H. Gu and L. Yang, *Polym. Eng. Sci.*, 2018, **58**, 1888–1900.
151 G. Gonzalez, A. Chiappone, I. Roppolo, E. Fantino, V. Bertana, F. Perrucci, L. Scaltrito, F. Pirri and M. Sangermano, *Polymer*, 2017, **109**, 246–253.
152 S. Arai, S. Tsunoda, A. Yamaguchi and T. Ougizawa, *Opt. Laser Technol.*, 2019, **113**, 345–356.
153 L. W. McKeen, in *Fatigue and Tribological Properties of Plastics and Elastomers*, William Andrew Publishing, 2nd edn, 2010, pp. 149–173.
154 A. Arzak, J. I. Eguiazábal and J. Nazábal, *J. Macromol. Sci., Phys.*, 1997, **36**, 233–246.
155 M. Roskies, J. O. Jordan, D. Fang, M. N. Abdallah, M. P. Hier, A. Mlynarek, F. Tamimi and S. D. Tran, *J. Biomater. Appl.*, 2016, **31**, 132–139.
156 W. Wu, P. Geng, G. Li, D. Zhao, H. Zhang and J. Zhao, *Materials*, 2015, **8**, 5834–5846.
157 X. Deng, Z. Zeng, B. Peng, S. Yan and W. Ke, *Materials*, 2018, **11**(2), 1–11.
158 M. Rinaldi, T. Ghidini, F. Cecchini, A. Brandao and F. Nanni, *Composites, Part B*, 2018, **145**, 162–172.
159 A. Sviridov, I. Lopatina and I. Kurganova, *IOP Conf. Ser.: Mater. Sci. Eng.*, 2019, **589**, 012021.
160 T. J. Hoskins, K. D. Dearn and S. N. Kukureka, *Polym. Test.*, 2018, **70**, 511–519.
161 I. Blanco, M. Rapisarda, S. Portuesi, G. Ognibene and G. Cicala, *AIP Conf. Proc.*, 2018, **1981**, 202181.
162 G. V. Salmoria, J. L. Leite and R. A. Paggi, *Polym. Test.*, 2009, **28**, 746–751.
163 N. A. Charoo, S. F. B. Ali, E. M. Mohamed, A. Mathew, T. Ozkan, M. A. Khan, Z. Rahman, N. A. Charoo, S. F. B. Ali, E. M. Mohamed and A. Mathew, *Drug Dev. Ind. Pharm.*, 2020, 1–9.
164 A. Golbang, E. Harkin-Jones, M. Wegrzyn, G. Campbell, E. Archer and A. McIlhagger, *Addit. Manuf.*, 2020, **31**, 100920.
165 K. H. Tan, C. K. Chua, K. F. Leong, C. M. Cheah, P. Cheang, M. S. Abu Bakar and S. W. Cha, *Biomaterials*, 2003, **24**, 3115–3123.
166 M. Yan, X. Tian, G. Peng, D. Li and X. Zhang, *Compos. Sci. Technol.*, 2018, **165**, 140–147.
167 S. Singh, V. S. Sharma, A. Sachdeva and S. K. Sinha, *Mater. Manuf. Processes*, 2013, **28**, 163–172.
168 G. Cicala, A. Latteri, B. Del Curto, A. Lo Russo and G. Recca, *J. Appl. Biomater. Funct. Mater.*, 2017, **15**, 10–18.
169 Y. Shi, J. Chen, Y. Wang, Z. Li and S. Huang, *Proc. Inst. Mech. Eng., Part L*, 2007, **221**, 37–42.
170 H. C. H. Ho, I. Gibson and W. L. Cheung, *J. Mater. Process. Technol.*, 1999, **89–90**, 204–210.
171 X. Zhang, L. Chen, C. Kowalski, T. Mulholland and T. A. Osswald, *J. Appl. Polym. Sci.*, 2019, **136**, 1–9.
172 R. Kumar, R. Singh and I. P. S. Ahuja, *Measurement*, 2018, **120**, 11–20.
173 H. C. H. Ho, W. L. Cheung and I. Gibson, *Rapid Prototyp. J.*, 2002, **8**, 233–242.
174 T. Serra, M. Ortiz-Hernandez, E. Engel, J. A. Planell and M. Navarro, *Mater. Sci. Eng., C*, 2014, **38**, 55–62.
175 S. XiaoHui, L. Wei, S. PingHui, S. QingYong, W. QingSong, S. YuSheng, L. Kai and L. WenGuang, *Int. J. Adv. Manuf. Tech.*, 2015, **81**, 15–25.
176 M. R. Snowdon, A. K. Mohanty and M. Misra, *ACS Omega*, 2017, **2**, 6446–6454.
177 G. C. Onwubolu and F. Rayegani, *Int. J. Manuf. Eng.*, 2014, **2014**, 1–13.
178 A. Roschli, K. T. Gaul, A. M. Boulger, B. K. Post, P. C. Chesser, L. J. Love, F. Blue and M. Borish, *Addit. Manuf.*, 2019, **25**, 275–285.
179 I. Blanco, G. Cicala, G. Ognibene, M. Rapisarda and A. Recca, *Polym. Degrad. Stab.*, 2018, **154**, 234–238.
180 K. R. Hart, R. M. Dunn and E. D. Wetzel, *Adv. Eng. Mater.*, 2019, **1901184**, 1–7.
181 M. A. Dechet, J. S. G. Bonilla, L. Lanzl, D. Drummer, A. Bück, J. Schmidt and W. Peukert, *Polymers*, 2018, **10**(12), 1–22.
182 M. D. Torres, *Rheology*, 2017, **1**, 3–4.
183 E. O. Cisneros-lópez, A. K. Pal, A. U. Rodriguez, F. Wu, M. Misra, D. F. Mielewski, A. Kiziltas and A. K. Mohanty, *Materials Today Sustainability*, 2019, 100027.
184 D. Filgueira, S. Holmen, J. K. Melbø, D. Moldes, A. T. Echtermeyer and G. Chinga-Carrasco, *Polymers*, 2018, **10**(3), 1–15.
185 I. Karakurt and L. Lin, *Curr. Opin. Chem. Eng.*, 2020, **28**, 134–143.
186 P. Wang, B. Zou, H. Xiao, S. Ding and C. Huang, *J. Mater. Process. Technol.*, 2019, **271**, 62–74.
187 E. O. Ogunsona, A. Codou, M. Misra and A. K. Mohanty, *J. Polym. Environ.*, 2018, **26**, 3574–3589.
188 E. Erbas Kiziltas, A. Kiziltas and E. C. Lee, *Polym. Compos.*, 2018, **39**, 3556–3563.
189 J. Andrzejewski, J. Cheng, A. Anstey, A. K. Mohanty and M. Misra, *ACS Sustainable Chem. Eng.*, 2020, 1–37.
190 M. Franchetti and C. Kress, *Int. J. Adv. Manuf. Tech.*, 2017, **88**, 2573–2579.
191 F. Mami, J. P. Revéret, S. Fallaha and M. Margni, *J. Ind. Ecol.*, 2017, **21**, S37–S48.
192 Q. Wang, J. Sun, Q. Yao, C. Ji, J. Liu and Q. Zhu, *Cellulose*, 2018, **25**, 4275–4301.
193 B. Singh, R. Kumar and J. Singh, *Mater. Today: Proc.*, 2020, **2**(2), 1–6.
194 R. Singh, R. Kumar and I. Singh, *J. Thermoplast. Compos. Mater.*, 2020, 1–20.
195 N. Jayanth and P. Senthil, *Composites, Part B*, 2019, **159**, 224–230.
196 H. Chung and S. Das, *Mater. Sci. Eng., A*, 2006, **437**, 226–234.
197 W. Jing, C. Hui, W. Qiong, L. Hongbo and L. Zhanjun, *Mater. Des.*, 2017, **116**, 253–260.
198 Y. Guo, K. Jiang and D. L. Bourell, *Polym. Test.*, 2014, **37**, 210–215.
199 C. Oztan, S. Ballikaya, U. Ozgun, R. Karkkainen and E. Celik, *Appl. Mater. Today*, 2019, **15**, 77–82.
200 J. S. Youn, J. W. Seo, S. Han and K. J. Jeon, *RSC Adv.*, 2019, **9**, 19606–19612.
201 A. Y. Davis, Q. Zhang, J. P. S. Wong, R. J. Weber and M. S. Black, *Build. Environ.*, 2019, **160**, 106209.

202 J. Gu, M. Wensing, E. Uhde and T. Salthammer, *Environ. Int.*, 2019, **123**, 476–485.
203 Q. Zhang, M. Pardo, Y. Rudich, I. Kaplan-Ashiri, J. P. S. Wong, A. Y. Davis, M. S. Black and R. J. Weber, *Environ. Sci. Technol.*, 2019, **53**, 12054–12061.
204 A. A. M. Damanhuri, A. Hariri, M. H. F. M. Fauadi, M. A. Rizal and M. R. Omar, *J. Safety, Heal. Ergon.*, 2019, **1**(1), 1–6.
205 P. Azimi, D. Zhao, C. Pouzet, N. E. Crain and B. Stephens, *Environ. Sci. Technol.*, 2016, **50**, 1260–1268.
206 M. R. Khosravani and T. Reinicke, *Appl. Mater. Today*, 2020, **20**, 100689.
207 D. Reay, C. Ramshaw and A. Harvey, in *Process Intensification: Engineering for Efficiency, Sustainability and Flexibility*, Oxford, 2nd edn, 2013, pp. 27–52.
208 J. Jiang, X. Xu and J. Stringer, *Robot. Comput. Integr. Manuf.*, 2019, **59**, 317–325.
209 T. Peng, K. Kellens, R. Tang, C. Chen and G. Chen, *Addit. Manuf.*, 2018, **21**, 694–704.
210 A. C. Gowman, M. C. Picard, A. Rodriguez-uribe, M. Misra, H. Khalil, M. Thimmanagari and A. K. Mohanty, *BioResources*, 2019, **14**, 3210–3230.
211 M. R. Snowdon, A. K. Mohanty and M. Misra, *ACS Sustainable Chem. Eng.*, 2014, **2**, 1257–1263.
212 A. van Wijk and I. van Wijk, *3D Printing with Biomaterials: Towards a Sustainable and Circular Economy*, IOS Press, Am, 2015.
213 Ellen Macarthur Foundation, *Circular Economy System Diagram*, Ellen MacArthur Foundation, https://www.ellenmacarthurfoundation.org/circular-economy/interactive-diagram, accessed 22 May 2018.
214 N. A. Nguyen, S. H. Barnes, C. C. Bowland, K. M. Meek, K. C. Littrell, J. K. Keum and A. K. Naskar, *Sci. Adv.*, 2018, 1–16.
215 F. L. Garcia, V. A. da S. Moris, A. O. Nunes and D. A. L. Silva, *Rapid Prototyp. J.*, 2018, **24**, 1166–1177.
216 I. V. Muralikrishna and V. Manikam, in *Environmental Management: Science and Engineering for Industry*, ed. P. Jardim, Butterworth-Heinemann, Elsevier, BS Publications, Oxford, 2017, pp. 55–75.
217 J. Faludi, C. Bayley, S. Bhogal and M. Iribarne, *Rapid Prototyp. J.*, 2015, **21**, 14–33.
218 J. Ma, J. D. Harstvedt, D. Dunaway, L. Bian and R. Jaradat, *J. Cleaner Prod.*, 2018, **192**, 55–70.
219 M. K. Niaki, S. A. Torabi and F. Nonino, *J. Cleaner Prod.*, 2019, **222**, 381–392.
220 R. Song, L. Clemon and C. Telenko, *J. Ind. Ecol.*, 2018, **23**(3), 669–708.
221 J. Plocher and A. Panesar, *Mater. Des.*, 2019, **183**, 108164.
222 T. Phillips, S. Fish and J. Beaman, *Addit. Manuf.*, 2018, **24**, 316–322.
223 W. Zhang, M. Tong and N. M. Harrison, *Addit. Manuf.*, 2019, **28**, 610–620.
224 T. Van Gerven and A. Stankiewicz, *Ind. Eng. Chem. Res.*, 2009, **48**, 2465–2474.